1960

Incipient motion of solid particles in a two-dimensional flow field

Connayil Mani Jacob
Iowa State University

Mic 60-4898

JACOB, Connayil Mani. INCIPIENT MOTION OF SOLID PARTICLES IN A TWO-DIMENSIONAL FLOW FIELD.

Iowa State University of Science and Technology
Ph.D., 1960
Engineering, agricultural

University Microfilms, Inc., Ann Arbor, Michigan

INCIPIENT MOTION OF SOLID PARTICLES IN A TWO-DIMENSIONAL FLOW FIELD

by

Connayil Mani Jacob

A Dissertation Submitted to the
Graduate Faculty in Partial Fulfillment of
The Requirements for the Degree of
DOCTOR OF PHILOSOPHY

Major Subjects: Theoretical and Applied Mechanics
Agricultural Engineering

Approved:

Signature was redacted for privacy.

Signature was redacted for privacy.

In Charge of Major Work

Signature was redacted for privacy.

Signature was redacted for privacy.

Heads of Major Departments

Signature was redacted for privacy.

Dean of Graduate College

Iowa State University
Of Science and Technology
Ames, Iowa

1960

TABLE OF CONTENTS

INTRODUCTION

Flowing fluids have the ability to maintain solid particles in suspension and to transport them. This well known phenomenon is of importance in many industrial processes where solids are transported by liquids or gases, or where solids need to be mixed or separated from fluids.

The application of the principles of sediment transportation is important in the design and maintenance of irrigation channels, reservoirs and harbors. In the construction of hydraulic filled dams, the material is transported to and deposited in its final position by water. Considerable study has been carried out in the field of sediment transport in connection with the control and development of natural streams.

Many serious problems in engineering and agriculture can be traced to this phenomenon. Silting and scouring of streams, and sedimentation of reservoirs and lakes are a few of them. The serious problem of soil erosion has its origin in this phenomenon. According to the Encyclopaedia Britannica (2):

> ...Nearly every country in the world has an erosion problem. Millions of acres of once productive land have been ruined for agricultural purposes. In the United States alone, according to a survey made by Soil Conservation Service in 1934, more than 57,000,000 acres have been rendered worthless for farming. This is approximately equal to the total area of the two States, New York and Pennsylvania....

The questions, why and when do solid particles resting on the bed of a channel move, are basic to the understanding of sediment transportation. The movement of a solid particle

resting on the bed of a channel consists of two parts, namely a movement parallel to the bed and another at right angles to it. The component of the resultant force that causes motion parallel to the flow is termed drag and that at right angles to it, lift. In the present investigation only lift is considered, and the term incipient motion is used in the restricted sense to include only incipient upward motion.

The purpose of the present investigation is to determine the lift experienced by a cylindrical solid resting on the bed of a channel in which two dimensional flow exists. Lift as used here is the bouyant weight of the solid, that is, the weight of the solid in water. A technique is developed to determine lift and the factors that influence lift are examined.

REVIEW OF LITERATURE

One of the earliest studies related to the problem of sediment transportation consisted in an attempt to develop a formula for the critical velocity at which sediment resting on the bed of a channel is drawn into the flow in the channel. In 1753, A. Brahms developed such a formula, which was later independently developed by W. Airy (5, p. 35), that related critical velocity to the weight of sediment. In this formula,

$$V_{cr} = kW^{1/6} \qquad (1)$$

where

V_{cr} = the critical velocity at which sediment is drawn into the flow,

k = a coefficient, and

W = weight of the sediment when it is submerged in water.

This equation, widely known as the sixth power law, was developed analytically. The force exerted by the flowing water on a particle resting on the bed of a stream was equated to the frictional force resisting movement. The former was considered to be

$$Z \gamma \pi a^2 \frac{v_{cr}^2}{2g},$$

where

a = the radius of the particle, which is assumed to be spherical,

πa^2 = the area exposed to the effect of the flowing water,

v_{cr} = the critical velocity at which the movement begins,

γ = the specific weight of water, and

Z = the shape factor.

The frictional force was considered to be

$$\mu(\gamma_1 - \gamma)\ 4/3\ a^3,$$

where

$4/3\ \pi a^3$ = the volume of the particle,

γ_1 = specific weight of the material of the particle, and

μ = the coefficient of friction between the particle and the bed of the stream.

Lift was not considered among the list of forces.

In 1816, the French engineer, L. G. du Buat (5, p. 34) compiled a list of critical velocities for various types of soils. For example, according to this list, the critical velocity for sand was 21.6 cm/sec, and that for sea pebbles, about an inch in diameter or more, 65.0 cm/sec.

The next distinctive step in the solution of the sediment transport problem appears to be the development of the concept of a critical tractive force, or drag, exerted by the flowing water, under which solid particles at the bed of a channel begin to move. This tractive force was defined as the product of the water depth, the slope of the channel and the specific weight of the water. The expression for tractive force, as defined here, was developed analytically by considering the equilibrium of the water flowing between two sections of a channel. This drag, which has the dimensions of FL^{-2}, has

in recent years been identified as the boundary shear that is widely used in modern fluid mechanics.

A. Schoklitsch (5, p. 42), one of the strong supporters of the drag theory, has listed the critical drag for various channel bed materials. For example, the critical drag for ordinary quartz sand 0.2 mm to 0.4 mm in diameter was listed as 0.18 to 0.20 kilograms per square meter.

Using this theory, scientists in many parts of the world have measured critical drag under various conditions and have applied these measurements to practical problems. According to experiments carried out at the U.S. Waterways Experiment Station, Vicksburg, Miss., the critical tractive force for the lower Mississippi was 0.25 pounds per square foot of river bed surface. G. H. Matthes (6) stated that the use of this value of drag gave satisfactory results when applied to important dredging operations in that part of the Mississippi.

One of the most well known experiments in sediment transport was carried out by A. Schields (11, p. 156). He introduced Prandtl's concept of the boundary layer into the analysis of the drag problem. He worked with dimensionless groups of variables and plotted on a logarithmic graph

$$\frac{\tau_c}{[\gamma_1 - \gamma]d} \text{ vs } \frac{d}{\delta},$$

where

τ_c = critical drag,

γ_1 = specific weight of solid particles,

γ = specific weight of water,

d = diameter of solids, and

δ = thickness of the laminar sublayer.

From the logarithmic plot he obtained the functional relationship,

$$\frac{\tau_c}{(\gamma_1-\gamma)d} = \phi\left(\frac{d}{\delta}\right) = \beta \approx 0.04,$$

where

β = a coefficient, which is very nearly constant.

Since this chart is considered an important contribution to the transport theory, it is shown in Fig. 1.

C. M. White (12) tested the equilibrium of sand grains on the bed of different types of conduits and reported his findings in 1939. By using oil and water for his liquids in addition to different types of conduits, he obtained a wide variety of experimental conditions. He showed that the drag required to start movement of grains was different for the two cases of low and high velocities of flow. He stated:

> ...At slow speeds and with small grains the pressure at the front of the grain does not appreciably exceed that at the rear....At high speeds and with larger grains such tangential drag becomes relatively unimportant compared with the drag due to pressure differences; the pressure distribution is not symmetrical but is less over the down stream half of the grain, so that when integrated it gives rise to a resultant force or form drag whose component resists motion....

He determined the drag required to start movement for the

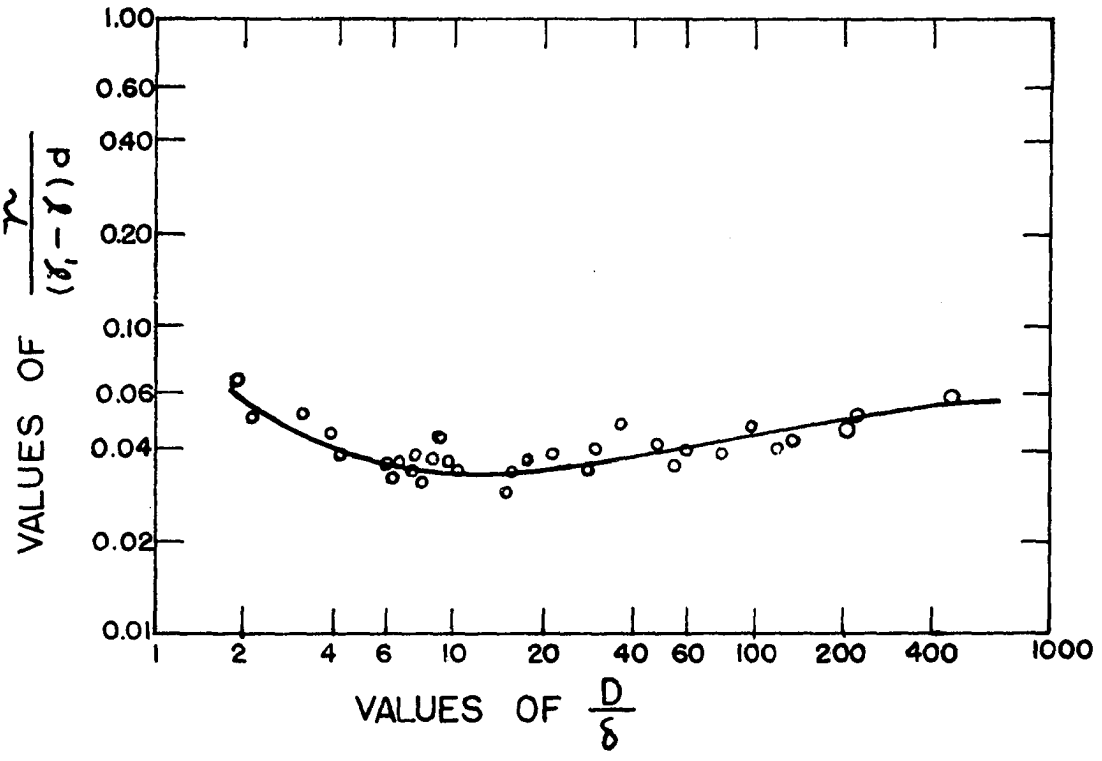

Fig. 1. Critical drag parameter vs. ratio of grain diameter to thickness of laminar layer.

two conditions stated above. Further, by designing a nozzle in which the drag was constant but the velocity was decreasing and observing that the grains moved simultaneously for the entire length of the nozzle, he concluded that the criterion for movement was drag and not velocity as implied in the sixth power law. Regarding the lift, White had this to say:

> ...the lift component must here be negligibly small. To verify this an experiment was made....A test grain was modelled in wax,...and fastened to the end of a piece of cotton which carried the whole horizontal force on the grain. Despite the high speed the grain did not rise, and so the lift seems less than its weight, which was only 3% of that of an ordinary silica grain....

Although White was skeptical about the existence of any appreciable lift on solids resting on the bed of a channel, several other investigators report to the contrary. H. A. Einstein and El-Sayed A. El-Samni (1) arranged half spheres in hexagonal pattern on the bottom of a flume and measured the lift experienced by them as a pressure difference. They found this pressure difference equal to

$$\Delta P = C_L \frac{\rho V^2}{2} , \qquad (2)$$

where

C_L = the lift coefficient.

The lift coefficient was found to have a constant value of 0.178 when the velocity, V, was measured at one fifth of the radius of the spheres below their top.

W. W. Rubey (9) expressed the drag F, by the familiar impact formula,

$$F = C_1 D^2 \rho \frac{U_o^2}{2} \qquad (3)$$

where

C_1 = a coefficient,

U_o = the average velocity experienced by the grain,

D = diameter of the grain, and

ρ = the density of the grain.

He concluded that his analysis could predict the behavior of coarse grains, but the formula gave values of U that were much lower than that needed for fine material.

Harold Jeffreys (3) developed analytically an expression for the lift experienced by an infinitely long cylinder placed transversely at the boundary of a two dimensional flow. This expression based on the potential theory for idealized conditions will be referred to in detail later under the section on analysis.

D. F. Young (13) determined the lift experienced by a spherical solid placed at the bottom of a glass tube in which water was flowing. The reverse slope of the tube prevented movement of the solid along the bed. When the sphere just lifted off the bottom of the tube the component of its bouyant weight normal to the bed gave the lift. The lift thus found was of the same order of magnitude as the drag.

A purely empirical approach to the problem, started during the early part of this century, deserves mention here. Investigators using this method have accumulated extensive

data which are of considerable practical value, especially in the design and operation of irrigation channels. Starting with Kennedy and Lacey (4) in India, these investigators developed formulas for the so called "regime" channels in alluvial soils. A regime channel is one which maintains its original cross section during an annual cycle of seasons. On the basis of numerous observations these men developed equations of the form

$$v_o = CH^n \tag{4}$$

where

v_o = mean velocity of flow in the channel,

H = the depth of flow in the channel, and

n = an exponent.

These formulas have been used extensively and with success in India and Egypt in the design of "regime," or non-silting and non-scouring, channels. Although empirical in nature these formulas show the influence of depth on the sediment carrying capacity of channels.

THEORY

Harold Jeffreys (3) analyzed the lift experienced by a long circular cylinder resting on the flat bed of a deep stream, and with its axis perpendicular to the flow. This analysis is based on the assumption of an ideal fluid, and makes use of potential theory.

With the cylinder present in the stream the flow becomes two dimensional. The complex potential function for this case is

$$w = aU\pi \operatorname{Coth} \frac{\pi a}{z} \qquad (5)$$

where

a = the radius of the cylinder,

U = the general velocity of the fluid, that is, the velocity without the presence of the cylinder, and

$z = x + iy$, where x and y are the horizontal and vertical displacements from the line of contact (Fig. 2) and $i = \sqrt{-1}$.

That equation (1) is a suitable complex potential function may be shown as follows. The imaginary part of $w = 0$, when $y = 0$ and where $|z - ia| = a$. That is, the imaginary part vanishes for the bottom of the stream and on the cylinder. Therefore, the sections of these surfaces by the planes of flow constitute stream lines. Further when $|z|$ is great, w approximates Uz, so that the correct undisturbed velocity is given when differentiated with respect to z.

The velocity components in the horizontal and vertical

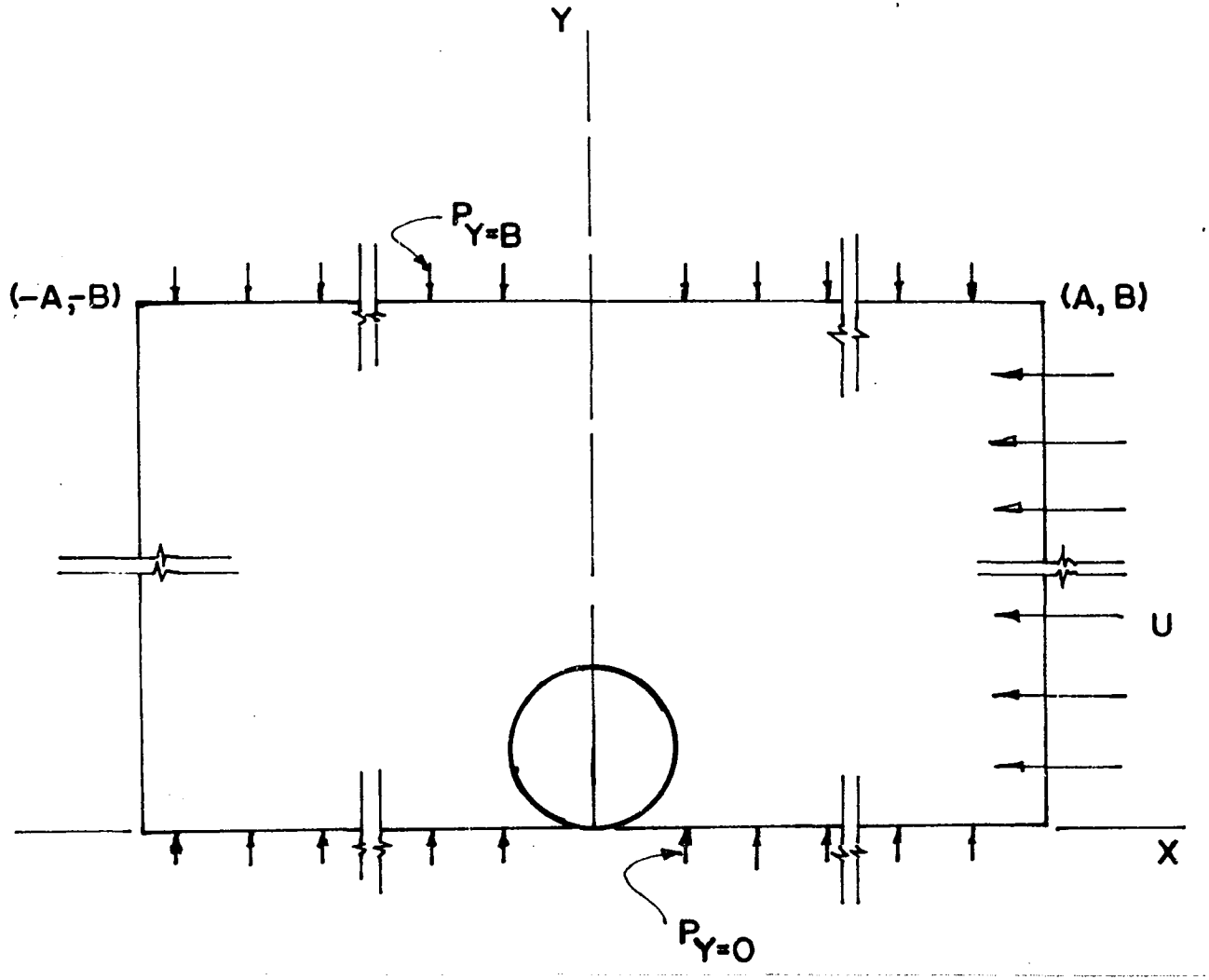

Fig. 2. Cross-section of a long cylinder resting on the flat bed of a deep stream.

directions, u and v are given by

$$u - iv = \frac{dw}{dz} = \frac{\pi^2 a^2 U}{z^2 \operatorname{Sinh}^2 \frac{\pi a}{z}} \qquad (6)$$

$$= \frac{U}{\left[\frac{x - iy}{\pi a} \operatorname{Sinh} \frac{\pi a}{x + iy}\right]^2} .$$

In the plane y = 0, this gives

$$u = \frac{U}{\left[\frac{x}{\pi a} \operatorname{Sinh} \frac{\pi a}{x}\right]^2} \quad \text{and } v = 0$$

and when $|z|$ is large

$$u - iv = U\left[1 - 1/3\left(\frac{\pi a}{z}\right)^2\right] + O(z^{-4})$$

$$= U .$$

This is obtained by expanding $\operatorname{Sinh} \frac{\pi a}{x}$ in series and simplifying.

Now consider a portion of the fluid bounded by the lines $x = \pm A$, $y = 0$ and $y = B$, where A and B are large and of the same order of magnitude, and a unit length in thickness (Fig. 2). The forces on the vertical sides have no vertical components. The upward thrust due to the pressures on the horizontal sides can be determined by using the Bernoulli equation:

$$p + g\rho z + 1/2\,\rho v^2 = \text{constant},$$

where

p = pressure,

ρ = density of fluid,

z = elevation, and

v = velocity of fluid.

For the present case this becomes

$$p + g\rho y + 1/2(u^2 + v^2) = \text{const.}$$

That is,

$$p = -g\rho y - 1/2(u^2 + v^2) + \text{const.} \qquad (7)$$

The upward thrust on the fluid due to the pressure on the horizontal sides is

$$\int_{-A}^{A} p\Big|_{y=0} dx - \int_{-A}^{A} p\Big|_{y=B} dx \quad \text{(Fig. 2).}$$

The contribution to this from the first term of equation (7) when no solid is present is

$$\int_{-A}^{A} - g\rho(0)dx - \int_{-A}^{A} - g\rho B\, dx = 2g\rho BA.$$

Because of the presence of the solid this exceeds the weight of the enclosed liquid by the weight of the water displaced by the solid, $\pi \rho a^2 g$. The contribution from the second term of equation (7) may be obtained as follows:

$$u^2 - v^2 = \frac{\pi^4 a^4 U^2}{z\bar{z}\ \mathrm{Sinh}^2 \frac{\pi a}{z}\ \mathrm{Sinh}^2 \frac{\pi a}{\bar{z}}} \quad . \qquad (8)$$

The term $\mathrm{Sinh}^2 \frac{\pi a}{z}\ \mathrm{Sinh}^2 \frac{\pi a}{\bar{z}}$ expanded in series and omitting terms involving higher orders of (1/B)

$$= \left[\left(\frac{\pi a}{x+iB}\right)^2 + \text{---}\right]\left[\left(\frac{\pi a}{x-iB}\right)^2 + \text{---}\right] = \frac{\pi^4 a^4}{x^2-B^2} - O(A,B).$$

Substituting these values and simplifying,

$$= -1/2\,\rho U^2 \int_{-A}^{A} \left[\left(\frac{x}{\pi a}\,\mathrm{Sinh}\,\frac{\pi a}{x}\right)^{-4} - 1\right] dx + O\left(\frac{1}{A} + \frac{1}{B}\right)$$

and when A and B are large this tends to

$$-\frac{1}{a}\rho U^2 \int_{-\infty}^{\infty} \left[\left(\frac{x}{\pi a}\,\mathrm{Sinh}\,\frac{\pi a}{x}\right)^{-4} - 1\right] dx. \qquad (9)$$

Since $x = 0$ is a singular point, equation (9) may be rewritten as

$$\frac{1}{2}\pi a \rho U^2 \int_{-\infty}^{0}\left[\left(\frac{1}{t^2} - \frac{t^2}{\mathrm{Sinh}^4 t}\right)\right] dt + \frac{1}{2}\pi a \rho U^2 \int_{0}^{\infty} \left(\frac{1}{t^2} - \frac{t^2}{\mathrm{Sinh}^4 t}\right. dt$$

$$= \pi a \rho U^2 \int_{0}^{\infty} \left(\frac{1}{t^2} - \frac{t^2}{\mathrm{Sinh}^4 t}\right) dt \qquad (10)$$

where $t = \frac{\pi a}{x}$ and $dt = -\frac{\pi a}{x^2}\,dx$.

This integral is

$$= \left[-\frac{1}{t} + \frac{1}{3}t^2\,\mathrm{Cosech}^2\,t\,\mathrm{Coth}\,t + \frac{1}{3}t\,\mathrm{Cosech}^2\,t + \frac{1}{3}\mathrm{Coth}\,t\right.$$

$$\left. - \frac{2}{3}t^2(\mathrm{Coth}\,t - 1)\right]_0^{\infty} - \frac{4}{3}\int_0^{\infty} (\mathrm{Coth}\,t - 1)\,t\,dt$$

$$= \frac{1}{3} + \frac{8}{3}\int_0^{\infty} t(e^{-2t} - e^{-4t} - e^{-6t} - \text{---})dt$$

$$= \frac{1}{3} + \frac{8}{3}\left(\frac{1}{2^2} + \frac{1}{4^2} + \frac{1}{6^2} + \text{---}\right)$$

$$= \frac{1}{3} + \frac{8}{3}\left(\frac{\pi^2}{24}\right) = \frac{1}{3} + \frac{1}{9}\pi^2 .$$

Therefore,

$$F - W = \pi \rho a^2 g + \pi \rho a U^2 \left(\frac{1}{3} + \frac{1}{9}\pi^2\right) \qquad (11)$$

where F = the upward thrust and W = the weight of the enclosed liquid. The upward thrust is transmitted to the solid. The solid will therefore be lifted off the bed of the stream if the right side of equation (11) exceeds the weight of the solid. If the density of the solid is ρ_1, this gives the required condition for incipient upward motion as

$$\pi \rho a \left[ga + U^2 \left(\frac{1}{3} + \frac{1}{9}\pi^2\right)\right] = \pi \rho_1 a^2 g , \qquad (12)$$

that is,

$$\left(\frac{1}{3} + \frac{1}{9}\pi^2\right) U^2 = \left[\frac{\rho_1 - \rho}{\rho}\right] ga . \qquad (13)$$

In expression (11) the term $\pi \rho a^2 g$ corresponds to the bouyant force on the solid. The second term $\pi \rho a U^2 \left(\frac{1}{3} + \frac{1}{9}\pi^2\right)$ thus represents the lift acting on the cylinder.

An ideal liquid was assumed in the development of equation (11). One dimensional flow was assumed in the undisturbed flow, the flow becoming two dimensional only after the introduction of the cylinder into the flow and the cylinder was

assumed to be infinitely long and the stream very deep. These assumptions are not valid for an actual case of a cylinder resting on the bed of a channel. Therefore, the experimental results for such a case is not expected to agree with the results obtained from equation (11).

DIMENSIONAL ANALYSIS

The forces involved in the phenomenon of sediment transportation are the drag and the list acting on the solid particles forming the sediment. Thus a study of the phenomenon consists of investigations of the drag and the lift. In this thesis lift is investigated. Discrete cylindrical solids were placed on the bed of a channel with their axes at right angles to the flow and the lift acting on them was studied. Two dimensional flow was maintained in the portion of the channel where the cylinders were placed.

The lift acting on a cylinder depends on several variables. The method of dimensional analysis has been used to study the relations among them. The variables which have been assumed to be pertinent in the phenomenon of lift, their symbols and fundamental dimensions are listed below.

Variable	Symbol	Dimension
1. Lift	L	F
2. Length of cylinder	l	L
3. Diameter of cylinder	d	L
4. Roughness of surface of cylinder	r_1	-
5. Roughness of channel bed	r_2	-
6. Slope of channel	S	-
7. Mean velocity of flow	v	LT^{-1}
8. Depth of flow	D	L
9. Viscosity of fluid	μ	FTL^{-2}
10. Density of fluid	ρ	FT^2L^{-4}

The function, using list as the dependent variable, may be written as

$$L = f(l, d, r_1, r_2, S, v, D, \rho, \mu) \tag{12}$$

The ten variables are expressed in terms of three fundamental dimensions, force, length and time. According to the Buckingham Pi theorem, the ten variables may be expressed in terms of 10 - 3 = 7 Pi terms. A Pi term as used in the theorem is a variable or a group of variables which is dimensionless, and independent of other variables or groups of variables (7). One possible set of Pi terms may be written as follows:

$$\pi_1 = \frac{L}{d^2v^2} \qquad \pi_2 = \frac{l}{d}$$

$$\pi_3 = \frac{D}{d} \qquad \pi_4 = r_1$$

$$\pi_5 = r_2 \qquad \pi_6 = S$$

$$\pi_7 = \frac{\rho vd}{\mu} .$$

Thus the function may be rewritten as

$$\frac{L}{\rho d^2v^2} = \phi_1 \left[\frac{l}{d}, \frac{D}{d}, r_1, r_2, S, \frac{\rho vd}{\mu}\right] . \tag{14}$$

That is,

$$\pi_1 = \phi_1 \left[\pi_2, \pi_3, \pi_4, \pi_5, \pi_6, \pi_7\right] . \tag{14a}$$

In order to get a function relating π_1 to the other Pi terms, experiments should be carried out to determine the influence on π_1 of each of the other Pi terms. The influence of π_2 on π_1 is obtained by varying π_2, keeping π_3, π_4, π_5 and π_6 constant, and noting the corresponding change in π_1. In a similar manner the influence of each of the remaining Pi terms on π_1 may be obtained. An equation may be developed for each one of these cases. These may then be combined using the principles of dimensional analysis to develop the functional relationship between π_1 and the rest of the Pi terms. This relationship will, of course, give lift as a function of the original variables.

In the present investigation only π_3 and π_7 were varied. Pi terms 2, 4, 5 and 6 were held constant throughout. A value of four for $\frac{l}{d}$ was arbitrarily chosen. All the cylinders tested had the same degree of surface roughness since they were all machined to size in exactly the same manner. The use of a plexiglass lining for the channel bed assured that r_1 was kept constant. The channel was maintained horizontal, thereby keeping S constant.

EXPERIMENTAL INVESTIGATION

The experimental investigation consisted of developing a technique for determining lift, and taking suitable observations when the upward motion of the cylinder resting on the bed of a channel was incipient. The free body diagram of a discrete cylinder resting on the bed of a channel and as tested in the present investigation is shown in Fig. 3.

$$\Sigma F_x = 0 \qquad D = T,$$

where D = the drag, and T = the tension in the strings. At incipient upward motion the reaction of the channel bed on the cylinder becomes zero. For this condition,

$$\Sigma F_y = 0 \qquad W = L + B,$$

where W = the weight of the cylinder, B = the bouyant force, and L = the lift.

The lift experienced by the cylinder was equal to the bouyant weight of the cylinder at incipient upward motion. When the upward motion of the cylinder was incipient, the depth of flow and the temperature were noted. The velocity profile of the flow corresponding to this condition was also determined.

The experimental investigation was carried out in several rather distinct phases. Each phase is described under the following subheadings.

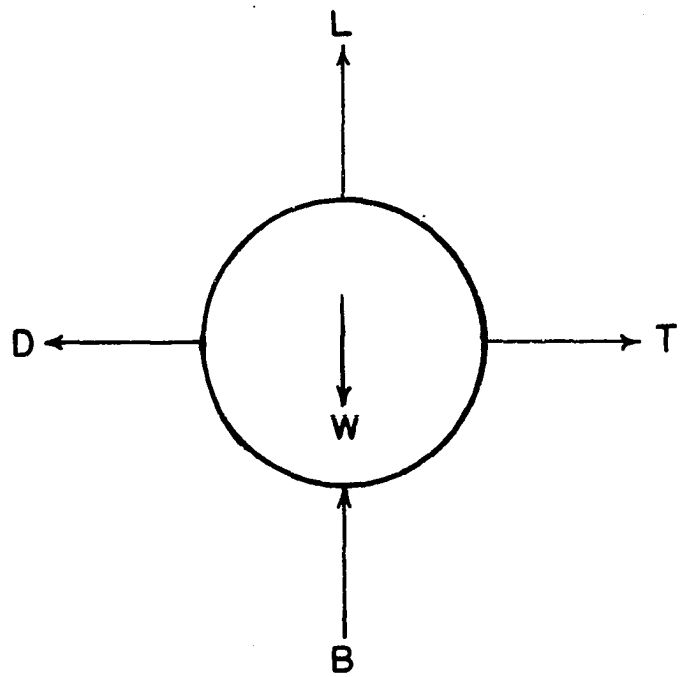

W = WEIGHT OF CYLINDER

B = BOUYANT FORCE

T = TENSION IN THE STRINGS

D = DRAG

L = LIFT

Fig. 3. Free body diagram of a cylinder under test.

Equipment

The main equipment consisted of an open channel 12 feet long by 6 inches wide by 15 inches deep. Originally the bottom of the channel was a standard steel I-section placed with its web parallel to the ground. Glass plates in lengths of 3 feet were attached to each flange in such a way that the plates were inside the flanges and extended down to the web, the bed of the channel. This bed of the channel was built up with cement concrete so that it was level with the top of the flange. Plexiglass sheets, 1/16 inch in thickness, were glued to the top of the cement concrete using Duco Cement. The sheets were also screwed to wooden plugs buried at five locations in the cement concrete. Thus a smooth bed, whose top could be seen without any obstruction through the glass sides of the channel, was obtained.

The channel was mounted on a frame so that the bed of the channel was about 30 inches from the ground. The frame was supported on legs which could be raised or lowered, so that it was possible to keep the bed of the channel at a desired slope.

A zero slope for the channel bed was maintained for the present investigation.

The water flowing in the channel was recirculated by a centrifugal pump and appropriate pipe connections. The flow in the channel was regulated by a valve placed on the discharge side of the pump. It was observed that for the range covered in the investigation the pump maintained a steady discharge and thus steady flow in the channel. The use of baffles at the entrance to the channel helped maintain a uniform flow over the part of the channel where the investigation was undertaken. Fig. 4 shows a photograph of the channel.

A tailgate, whose height could be controlled manually, was provided at the discharge end of the channel. This made it possible to adjust the depth of flow in the channel for a given discharge. Six different tailgate settings were used in the present investigation.

Selection of Cylindrical Solids

It was desired to choose solids whose specific weights were slightly more than that of water. Two such materials were used in preparing the cylindrical specimens. One of the materials was a clear white plastic. A one half inch diameter rod of this material was procured and six sizes of cylinders having diameters of 0.325 in., 0.300 in., 0.275 in., 0.250 in., 0.225 in. and 0.200 in. were prepared by turning the original rod down on a lathe to the required dimensions. The material

Fig. 4. The rectangular open channel used for investigation.

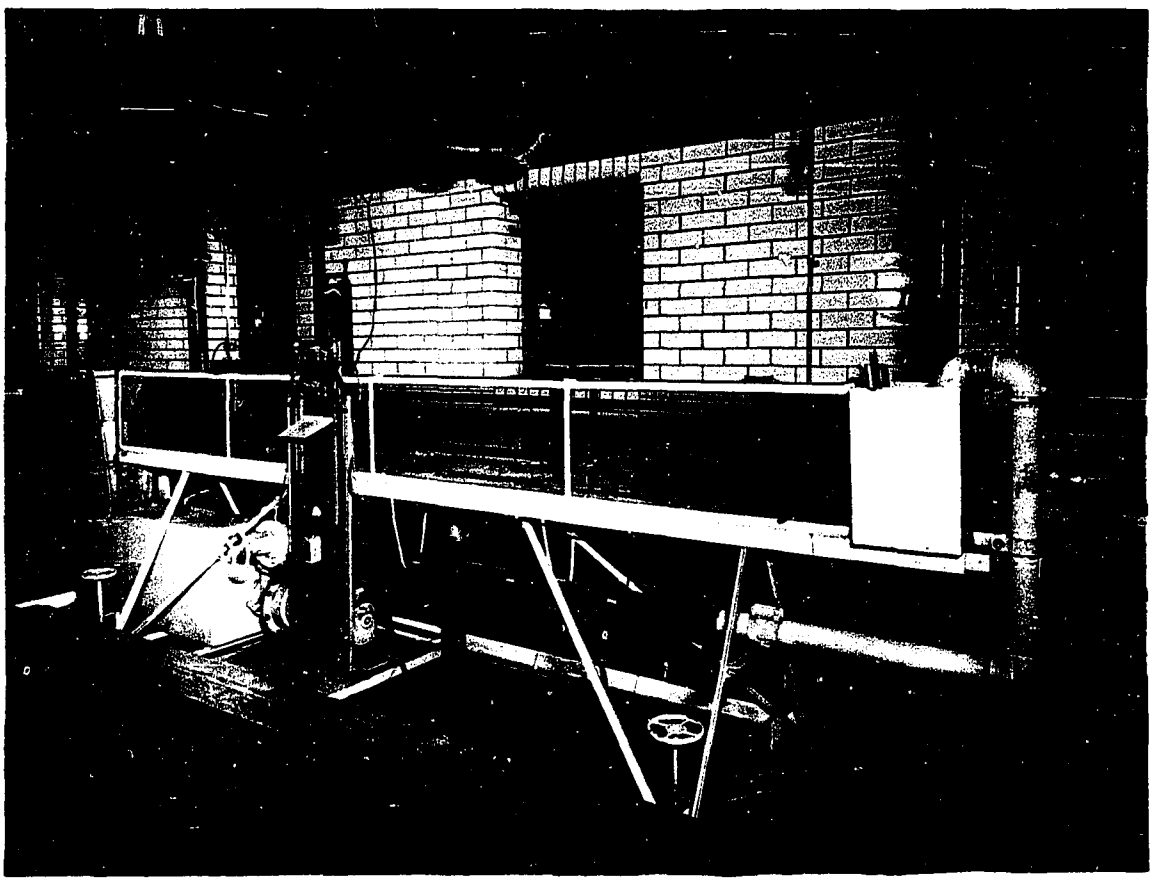

had an average specific gravity of 1.05.

The other material was made in the laboratory by curing polyester resin with a catalyst. The cured resin which was in liquid form at first was poured into a half-inch diameter glass tube taking care that no entrapped air remained in the liquid. It was observed that when smaller sizes of tubes were used it was difficult to force out all of the entrapped air. In twenty-four hours time the liquid hardened into a solid rod. The solid material thus developed had an average specific gravity of 1.20.

Five different cylinders having diameters of 0.325 in., 0.300 in., 0.275 in., 0.250 in. and 0.225 in. were prepared out of this rod in exactly the same manner as the cylinders from the other material. Since the manner of preparation of the specimens from both the materials was the same, it was assumed that they all had the same surface roughness.

A constant ratio of length of a cylinder to its diameter of four was arbitrarily chosen for each cylinder. These specimens are shown in Fig. 5.

Two symmetrical holes 0.80 in. apart were drilled in each cylinder along the diameter and transverse to its axis. Cotton threads 18 inches long were passed through these holes. Each thread was knotted at one end while the other end was tied to a needle. Thus it was possible to place the cylinders at right angles to the flow and their position maintained by the needles when the latter were fixed to the bed of the channel.

Plastic cylinders, 0.325 in., 0.300 in., 0.276 in.,
0.250 in., 0.226 in. and 0.201 in. diameter.

Cured polyester resin cylinders, 0.325 in., 0.300 in., 0.276 in.,
0.250 in., and 0.226 in.
diameter

Fig. 5. Cylindrical specimens used for investigation.

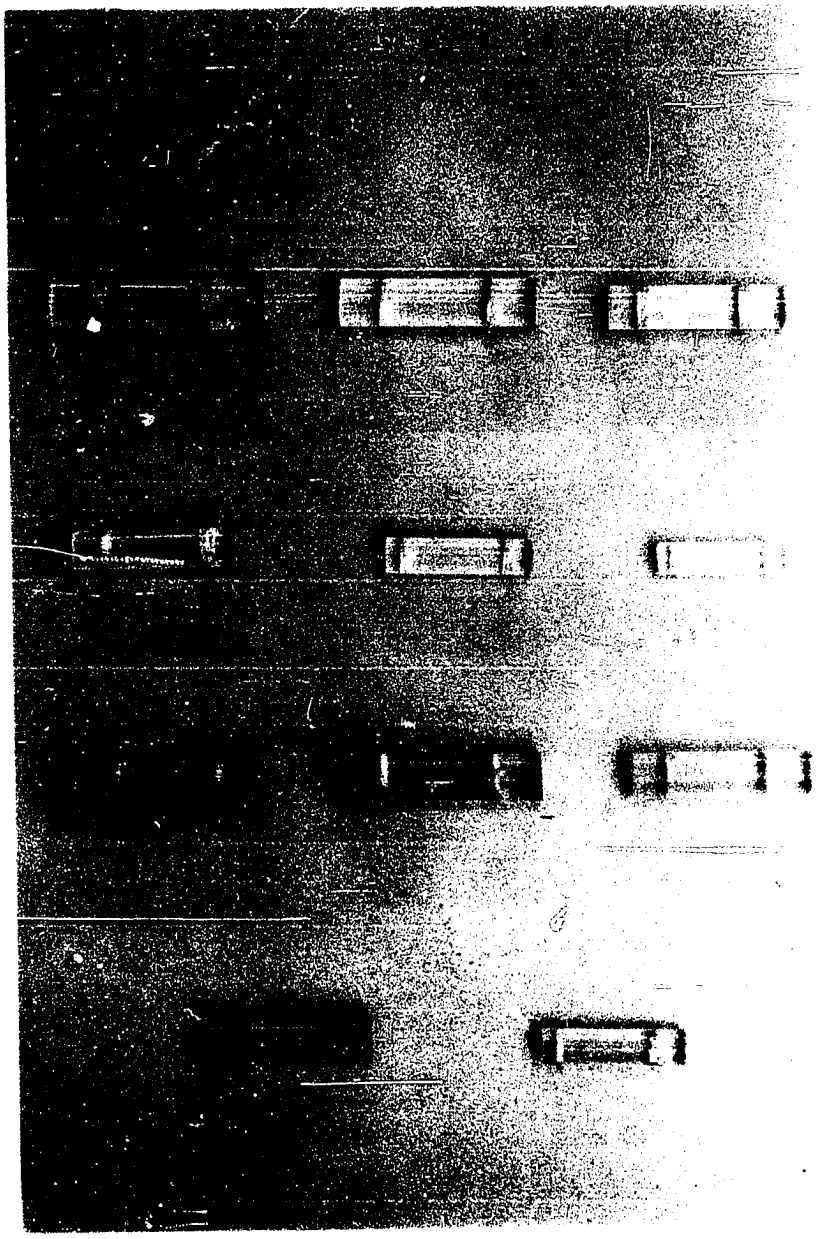

The arrangement for testing is shown in Fig. 6.

The cotton strings tied to the needles prevented any movement parallel to the channel bed. Thus the drag at all times was equalized by the tension developed in the strings.

The strings did not prevent any slight movement of the cylinder in a vertical direction. At incipient upward motion, the tension in the strings has no vertical component. Thus the lift at incipient motion is given by the weight of the cylinder minus the bouyant force on the cylinder. This is the same as the weight of the cylinder in water.

The length and diameter of a cylinder were determined by measuring with a micrometer. The specific gravity was determined by weighing each cylinder in air and in water and dividing the former by the difference between the two weights. The average for all the cylinders of one material was taken as the specific gravity for that material.

Velocity Measurement and Determination of Velocity Profile

The velocity at a specific location in the flow was measured using a pitot tube connected to a micromanometer. The pitot tube used in the present investigation allowed velocity measurements to be taken as close as 1/8 inch to the bed of the channel. The micromanometer could be read to one-thousandth of an inch. Carbon tetrachloride having a specific gravity of 1.595 was used as the gage fluid. This gave the expression for the velocity in terms of the differential

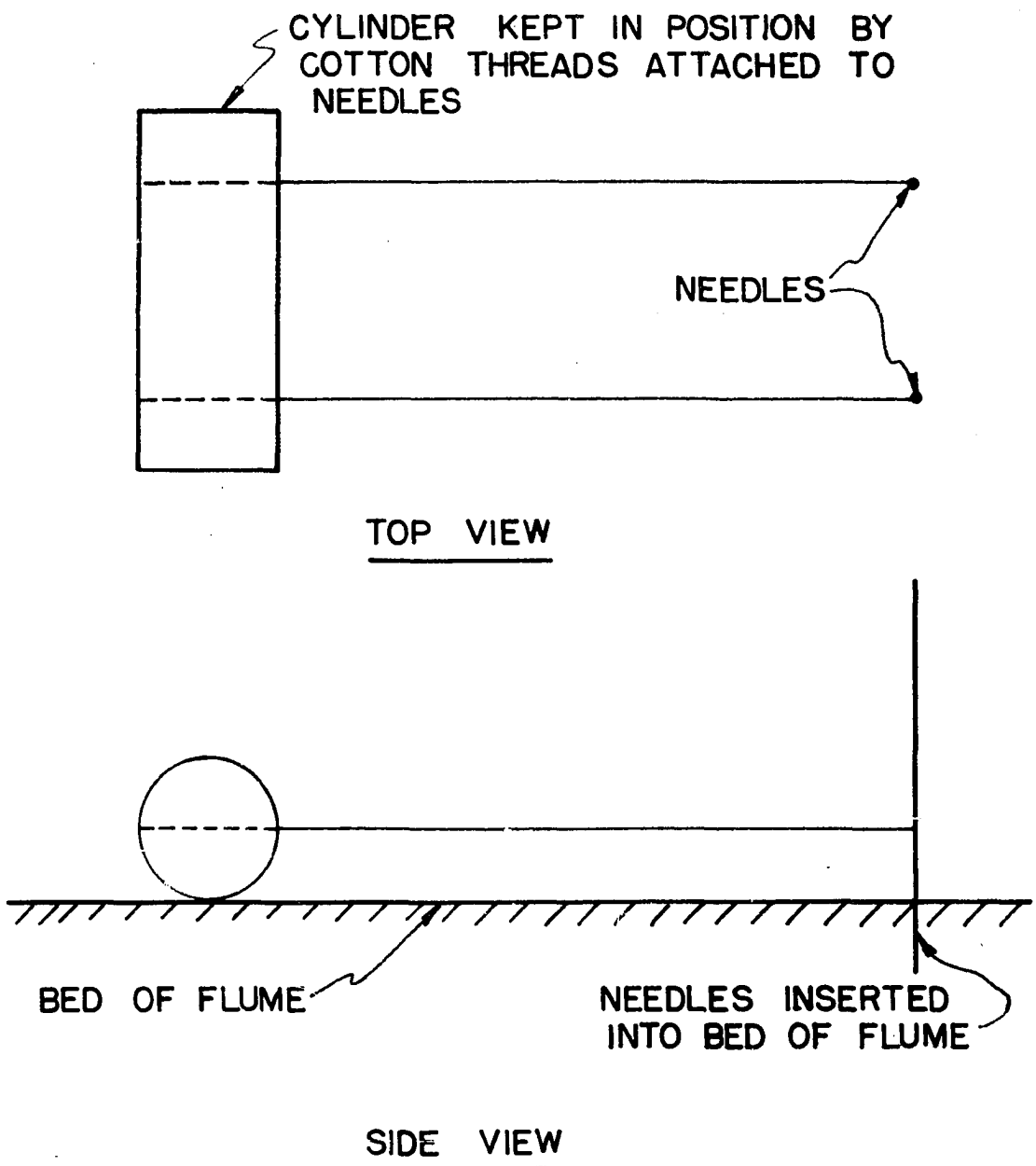

Fig. 6. Arrangement of a cylinder for testing.

reading of the manometer as

$$v = 1.79\sqrt{H}$$

where v = the velocity in fps and H = the differential manometer reading in inches of gage fluid. Fig. 7 shows the pitot tube and manometer used for measuring velocity.

The velocity profile at the required location was determined by measuring velocities at several points lying on a vertical line. The first measurement was taken at 0.010 ft. from the bed of the channel, the next one at 0.020 ft. from the bed of the channel, the next at 0.040 ft. and the subsequent ones at distances of either 0.020 ft. or 0.040 ft. from the previous point. The 0.020 ft. distance between points after the 0.040 ft. reading was used for depths of flow less than 1.40 in., while the 0.040 ft. distance was used when the depth was greater. Thus between six to ten micromanometer readings were taken for depths between about 1.0 in. to 2.5 in. in order to determine the velocity profile.

Depth Measurement

The depth of flow in the channel was measured by a point gage that read to one-thousandth of a foot. The gage was fixed to the top of the steel frame supporting the open channel in such a way that the pointer moved in a vertical direction. The difference between the readings when the pointer was touching the bed of the channel and the surface

Fig. 7. Manometer used for measuring velocity.

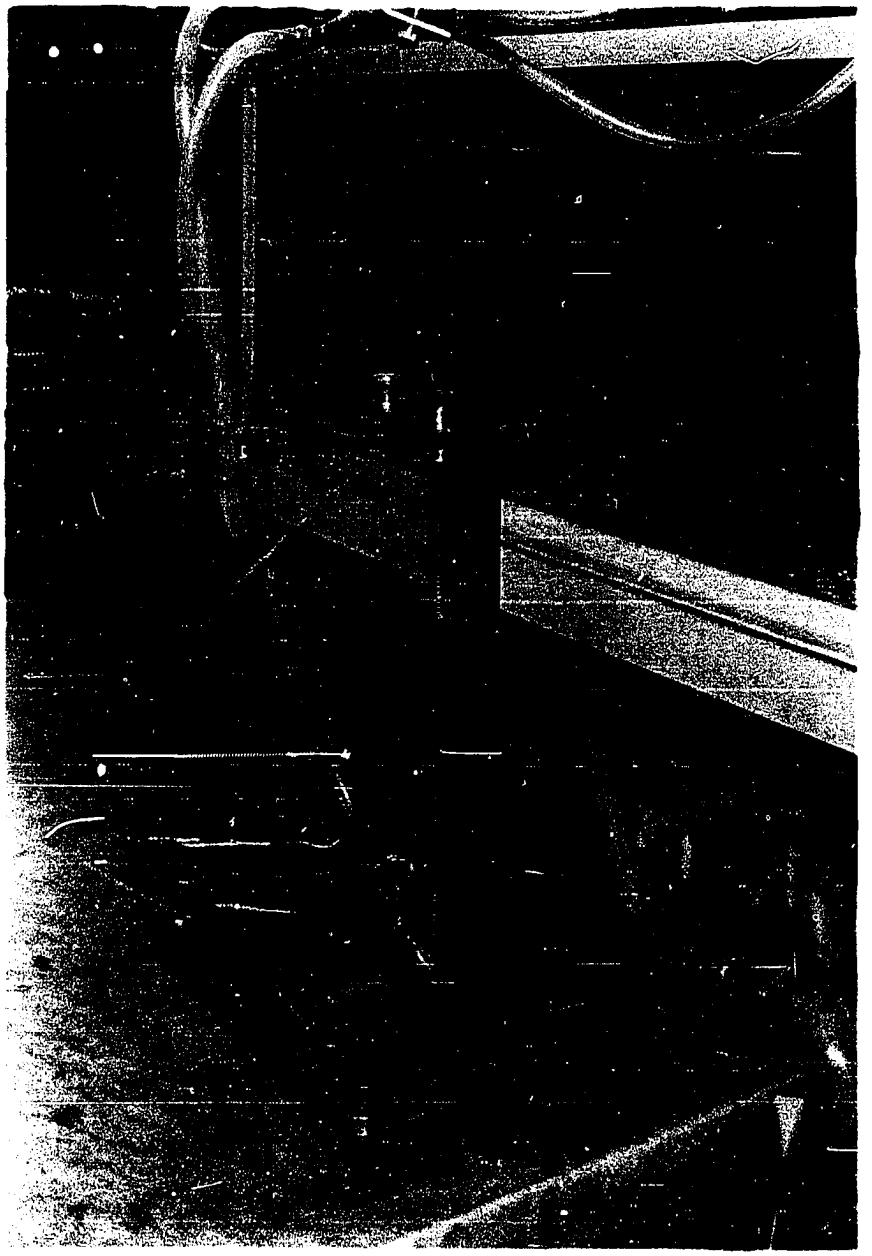

of the water gave the depth of flow in the channel. The arrangement of the point gage with respect to the channel is shown in Fig. 8.

The point gage was also used for locating the position of the pitot tube. The point gage was set at the required reading and then the pitot tube was brought with its center in line with the tip of the pointer. After the pitot tube was fixed in position the pointer was removed from the flow.

Experimental Procedure

Establishment of two dimensional flow

It is clear that two dimensional flow could exist only in those portions of the channel where the boundary effects of the sides become negligible. In order to ascertain the region of two dimensional flow, velocity profiles were taken at several locations across the channel. Measurements were taken forty inches from the tailgate where all the cylinders were tested and at another location eighteen inches upstream from it (Appendix). From the velocity profiles thus determined two conclusions were drawn. First of all it was concluded that the central two inches of flow was two dimensional, and secondly, uniform flow existed for a sufficient length of the channel. All of the experimental investigation was confined to this portion of the channel.

Placement of the cylinder in the channel

Each cylinder was placed on the bed of the channel with

Fig. 8. The point gage for measuring the depth of flow.

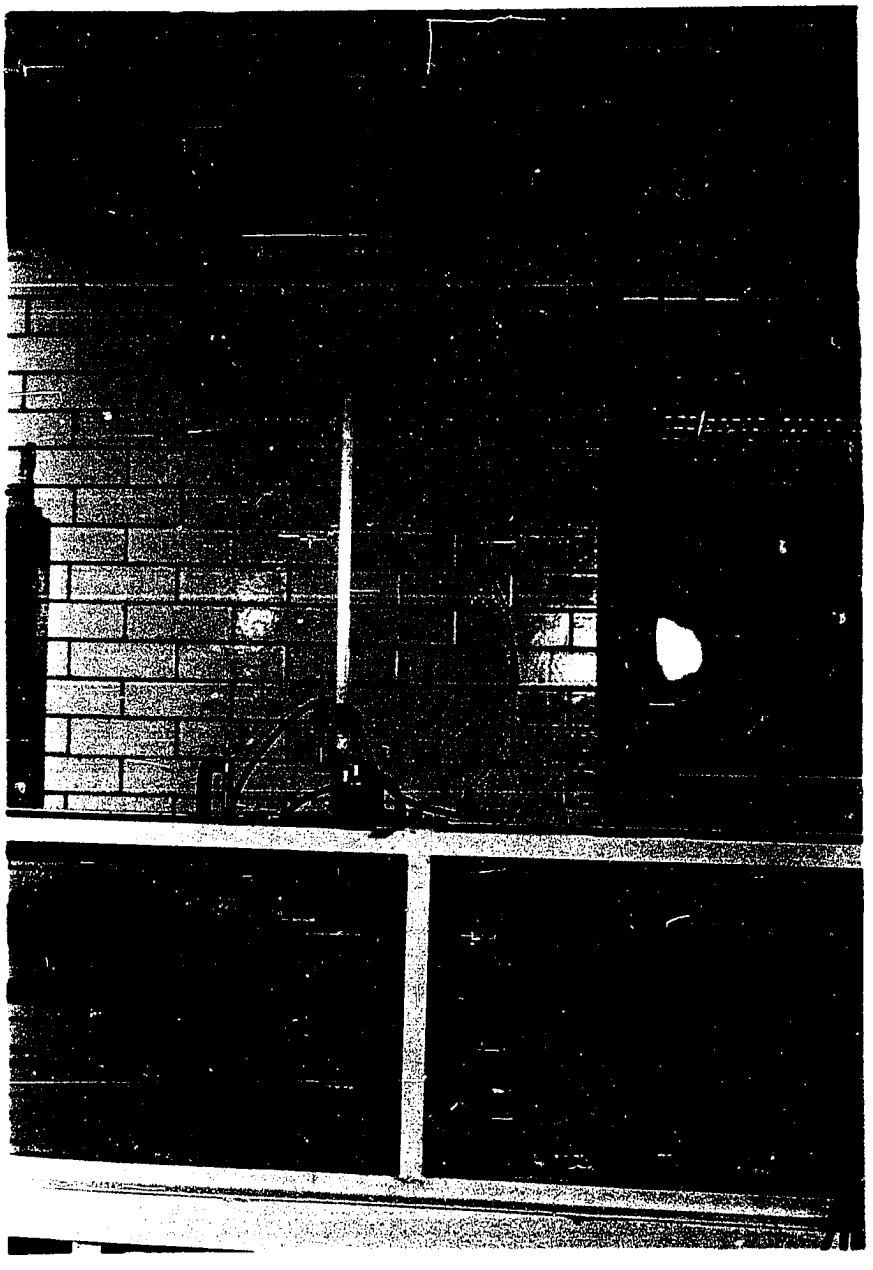

its axis at right angles to the longitudinal axis of the channel and symmetrical to it. The cylinders were placed forty inches from the tailgate where the flow was found to be uniform. Each cylinder was held in position by two cotton threads which attached the cylinder to the two needles. The two needles were inserted into the bed of the channel in such a way that the threads remained parallel to each other, were symmetrical about the longitudinal axis of the channel and horizontal.

Incipient upward motion

The tailgate was then set at a desired height and the pump started. When the rate of flow was low the cylinder remained motionless on the bed of the channel. Any drag experienced by the cylinder was counterbalanced by the tension developed in the strings. As the rate of flow was increased, at a certain stage, the solid started to bounce up and down on the bed of the channel. The bouncing became quite rapid as the flow was further increased.

The incipient upward motion of a cylinder was taken to correspond to the first observable bouncing of the solid on the bed of the channel. Since the cylinder is originally at rest, it must accelerate in order to initiate movement. Only when the acceleration in the vertical direction tends to zero will the lift be equal to the bouyant weight of the cylinder. Thus the lift experienced by the cylinder must have been greater than the weight of the cylinder in water. An estimate

of the error involved was made assuming the bouncing motion of the cylinder to be simple harmonic. When the inertia force was thus taken into account, the error involved was about three per cent for the heaviest cylinder.

Tests

Each cylinder was tested for six different tailgate settings. At incipient motion, indicated as explained earlier, the depth of flow was measured by the point gage. The temperature of the water was also noted. Observations of depth and temperature were repeated four times, twice as the flow was increased and twice as the flow was decreased. The average of the four depth readings was taken as the depth and the average of the four temperature readings, the temperature at critical conditions.

After the cylinders were tested, the flow conditions corresponding to incipient motion were simulated in the channel except for the temperature of water. However, the temperature difference between the two matched conditions of flow never varied more than three degrees centigrade. This was taken to be reasonably close since the variation of viscosity of water in the temperature range did not exceed two per cent. Measurements were then taken to determine the velocity profile for each case.

RESULTS

Development of the Equation of the Velocity Profile Curves

A total of eleven cylinders were tested for six different tailgate settings. Thus, theoretically, this should give 66 different conditions of flow corresponding to the incipient motion of the cylinders. However, it was actually observed that for a given tailgate setting the flow conditions at incipient motion of all the cylinders of one material coincided (Table 4, Appendix). Since there were six different tailgate settings and two different materials, a total of 12 different sets of flow conditions resulted. Data were taken to determine the velocity profile for each of these sets of flow conditions.

Figures 9 to 11 show three representative curves of y/D plotted against velocity on logarithmic paper, where y = distance in ft. from the bed of the channel and D = the depth of flow, for each set of flow conditions at incipient motion. These curves indicated that it was reasonable to assume a form of equation for the velocity profile curves as follows:

$$v = a\left(\frac{y}{D}\right)^{b} \tag{15}$$

where

v = the velocity in fps,

a = a coefficient,

y = the distance in ft. from the bed of the channel where the velocity is determined,

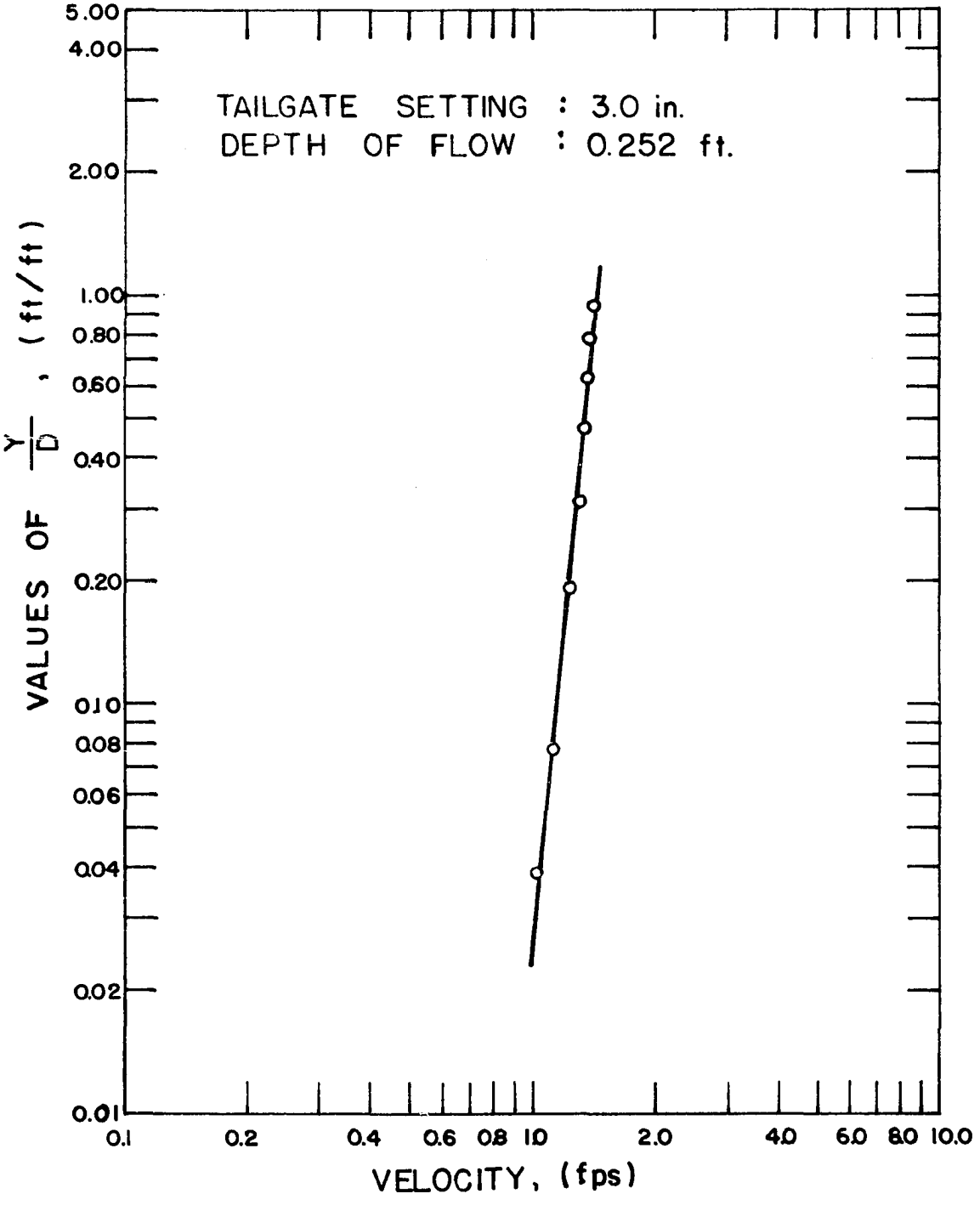

Fig. 9. $\frac{Y}{D}$ vs. velocity, where Y = distance from bed in ft.
D = depth of flow in ft.

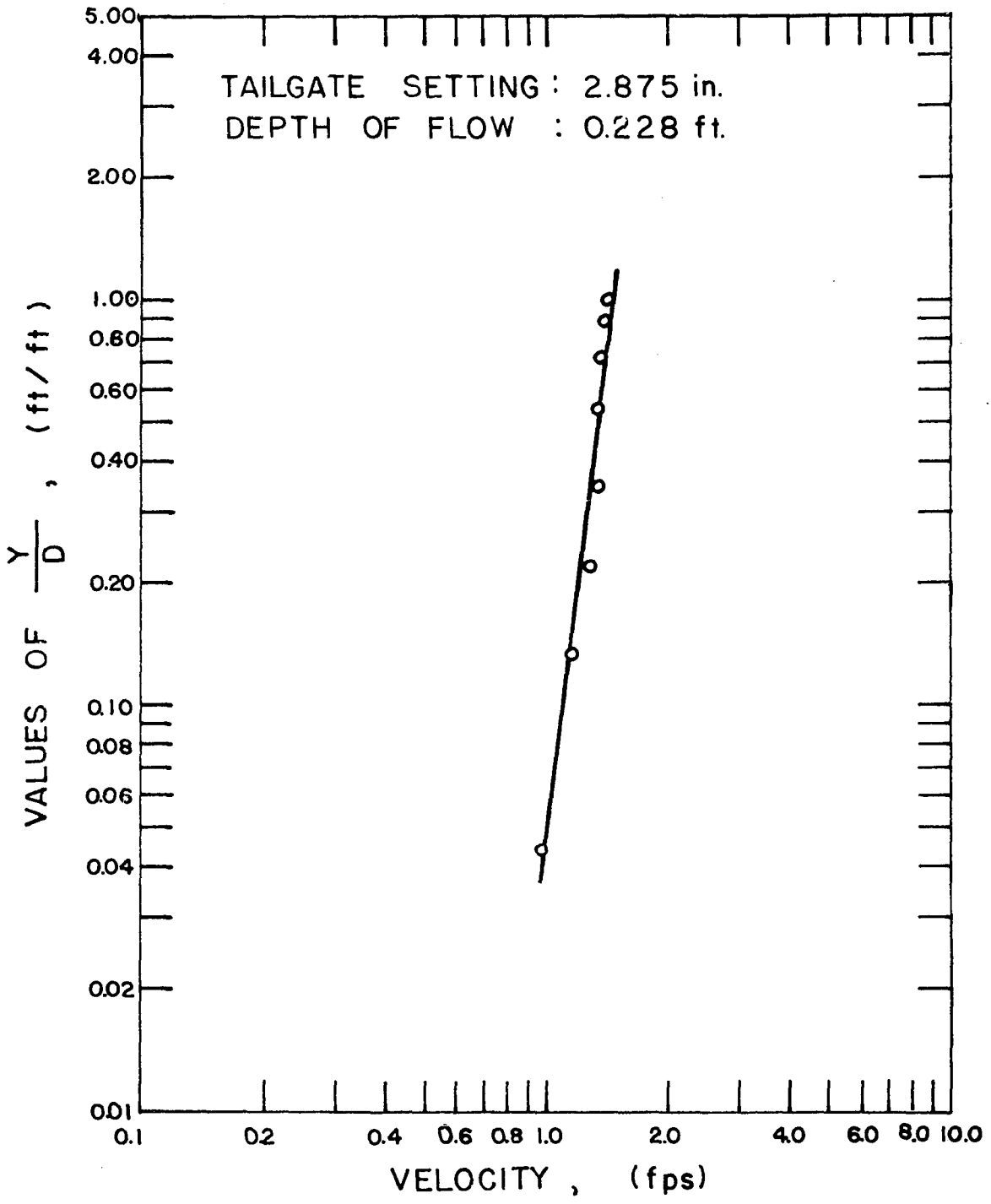

Fig. 10. Velocity profile. Y = distance from bed.
D = depth of flow.

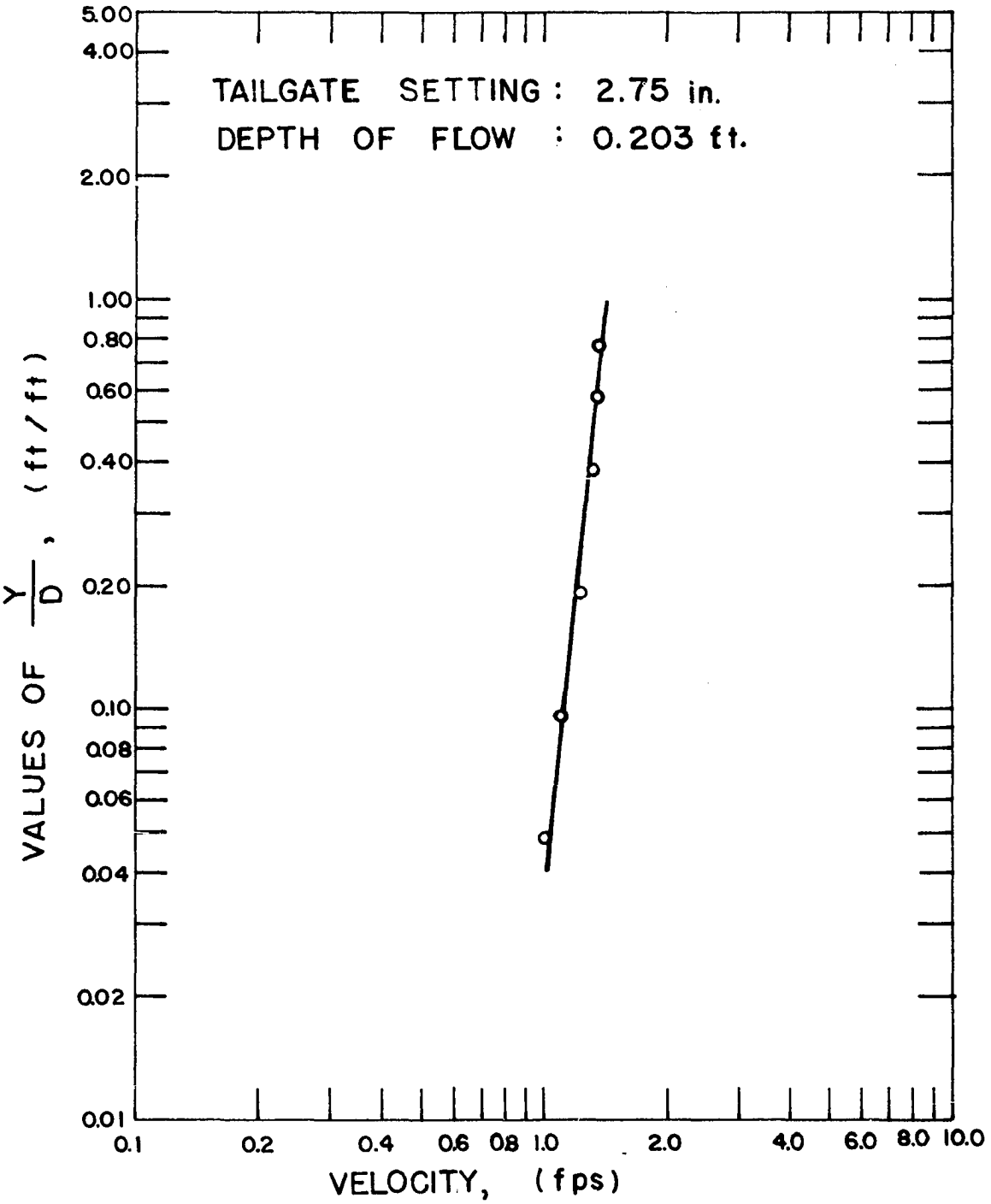

Fig. 11. $\frac{Y}{D}$ vs. velocity, where Y = distance from bed in ft.
D = depth of flow in ft.

Equation of the curve: $v = 1.447 \left(\frac{y}{D}\right)^{0.119}$.

Fig. 12. Velocity profile curve. Y vs. velocity, where
Y = distance from bed in ft.
Tailgate setting 3 in. and depth of flow 0.252 ft.

Equation of the curve: $v = 1.439 \left(\frac{y}{D}\right)^{0.109}$.

Fig. 13. Velocity profile curve. Y vs. velocity, where
Y = distance from bed in ft.
Tailgate setting $2\frac{7}{8}$ in. and depth of flow 0.228 ft.

Equation of the curve: $v = 1.398 \left(\frac{y}{D}\right)^{0.0821}$.

Fig. 14. Velocity profile curve. Y vs. velocity, where
Y = distance from bed in ft.
Tailgate setting $2\frac{6}{8}$ in. and depth of flow 0.203 ft.

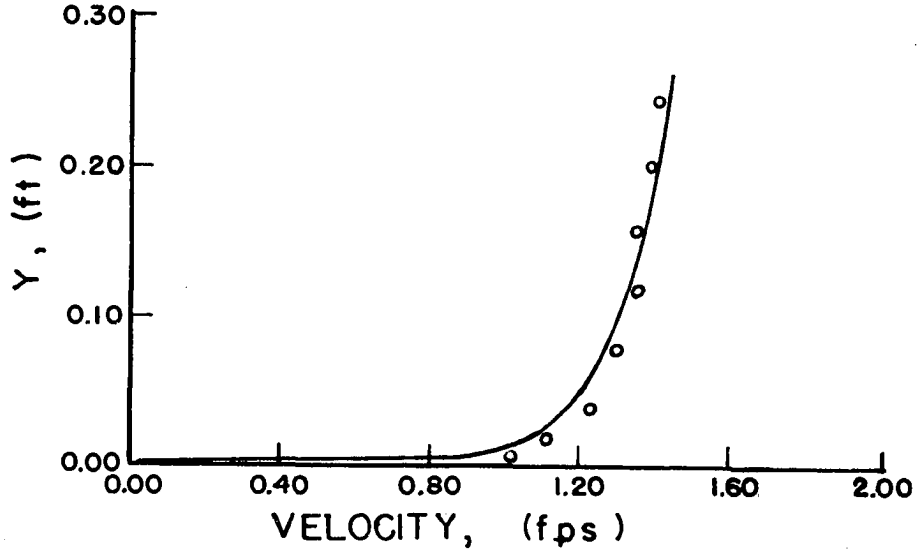
0.30
0.20
0.10
0.00
Y, (ft)
0.00
0.40
0.80
1.20
1.60
2.00
VELOCITY, (fps)

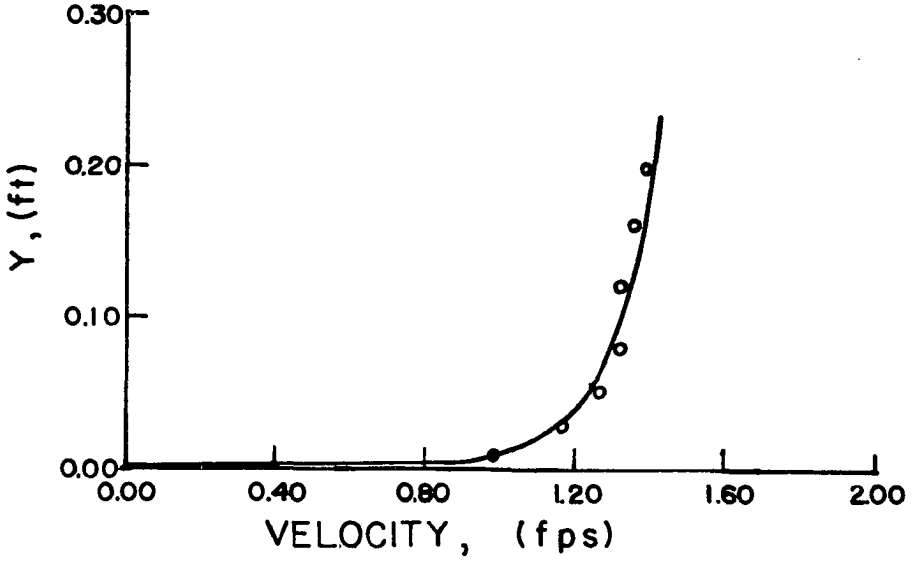
0.30
0.20
0.10
0.00
Y, (ft)
0.00
0.40
0.80
1.20
1.60
2.00
VELOCITY, (fps)

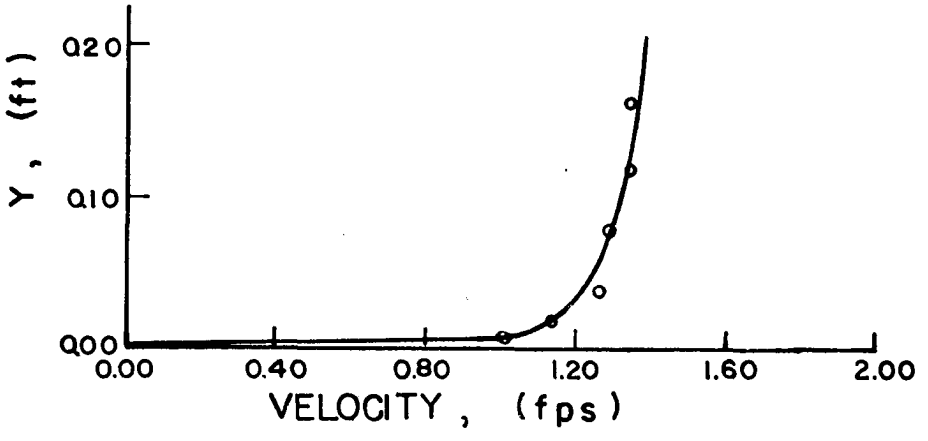
0.20
0.10
0.00
Y, (ft)
0.00
0.40
0.80
1.20
1.60
2.00
VELOCITY, (fps)

D = the depth of flow in ft., and

b = an exponent.

It was decided to fit a curve of this form to the data obtained for each velocity profile. Equations of such curves were developed using regression technique. Figures 12 to 23 show the velocity profile curves plotted according to these equations. The data from which each equation was developed are also shown in each figure. A sample set of calculations for the development of the equation for a velocity profile is given in Appendix

Determination of Significant Velocity

An important question in the analysis of lift is which is the significant velocity that influences lift. In order to establish the significant velocity it is necessary to consider different velocities and compare the results obtained from each of them. In the past investigators have used different velocities as significant. Some of these are the mean velocity of flow in the channel, the mean velocity of flow for a distance equal to the diameter of the solid, the velocity at the centroid of the solid, and velocities at distances from the bed of the channel which hold a constant ratio to the diameter of the solid. After preliminary trials with the mean velocity of flow for a distance equal to the diameter of the cylinder, the mean velocity of flow in the channel and the centroidal velocity, the latter two were chosen for

Equation of the curve: $v = 1.409 \left(\frac{y}{D}\right)^{0.119}$.

Fig. 15. Velocity profile curve. Y vs. velocity, where
Y = distance from bed in ft.
Tailgate setting 2 $\frac{5}{8}$ in. and depth of flow 0.184 ft.

Equation of the curve: $v = 1.298 \left(\frac{y}{D}\right)^{0.110}$.

Fig. 16. Velocity profile curve. Y vs. velocity, where
Y = distance from bed in ft.
Tailgate setting 2 $\frac{4}{8}$ in. and depth of flow 0.154 ft.

Equation of the curve: $v = 1.197 \left(\frac{y}{D}\right)^{0.0665}$.

Fig. 17. Velocity profile curve. Y vs. velocity, where
Y = distance from bed in ft.
Tailgate setting 2 $\frac{3}{8}$ in. and depth of flow 0.133 ft.

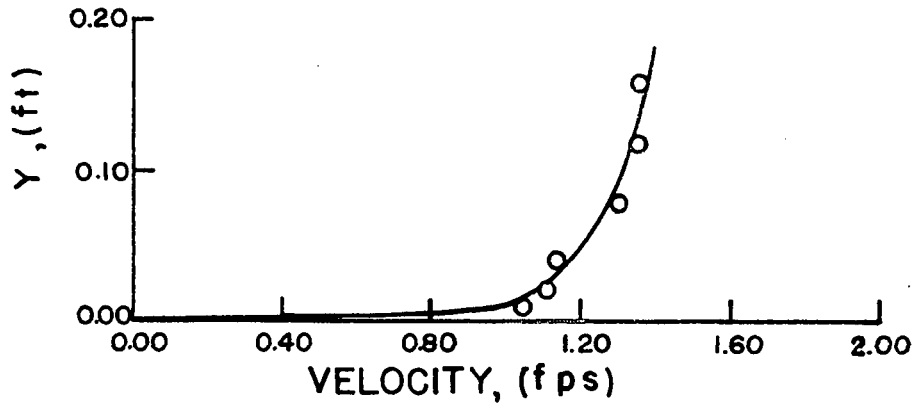
0.20
0.10
0.00
Y, (ft)
0.00
0.40
0.80
1.20
1.60
2.00
VELOCITY, (fps)

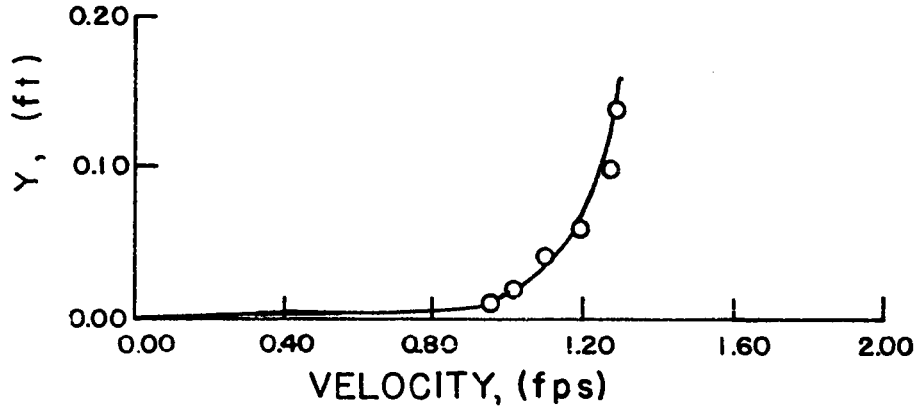
0.20
0.10
0.00
Y, (ft)
0.00
0.40
0.80
1.20
1.60
2.00
VELOCITY, (fps)

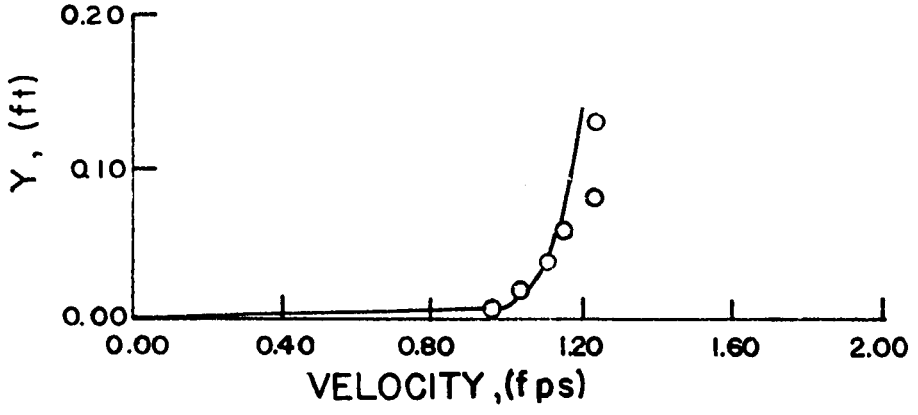
0.20
0.10
0.00
Y, (ft)
0.00
0.40
0.80
1.20
1.60
2.00
VELOCITY, (fps)

Equation of the curve: $v = 0.859 \left(\frac{y}{D}\right)^{0.109}$.

Fig. 18. Velocity profile curve. Y vs. velocity, where
Y = distance from bed in ft.
Tailgate setting 3 in. and depth of flow 0.184 ft.

Equation of the curve: $v = 0.853 \left(\frac{y}{D}\right)^{0.0975}$.

Fig. 19. Velocity profile curve. Y vs. velocity, where
Y = distance from bed in ft.
Tailgate setting $2\frac{7}{8}$ in. and depth of flow 0.165 ft.

Equation of the curve: $v = 0.854 \left(\frac{y}{D}\right)^{0.084}$.

Fig. 20. Velocity profile curve. Y vs. velocity, where
Y = distance from bed in ft.
Tailgate setting $2\frac{6}{8}$ in. and depth of flow 0.147 ft.

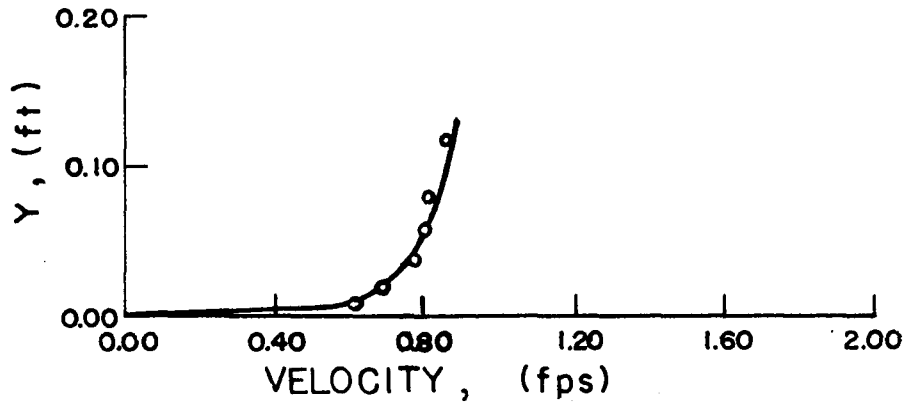
0.20
0.10
0.00
Y , (ft)
0.00
0.40
0.80
1.20
1.60
2.00
VELOCITY , (fps)

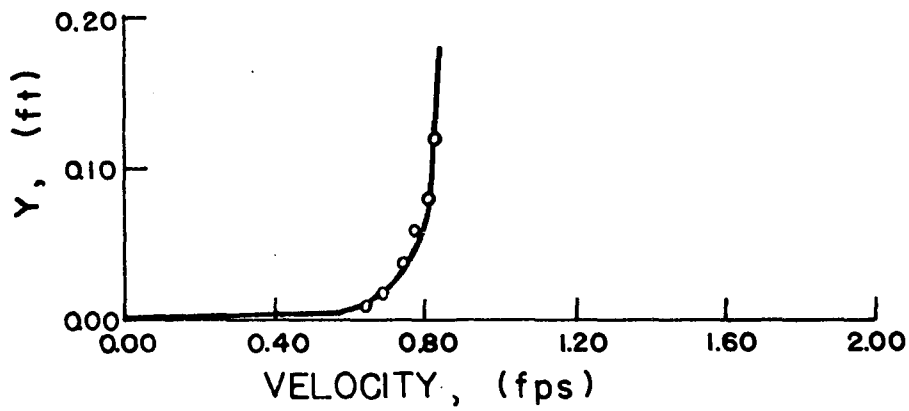
0.20
0.10
0.00
Y , (ft)
0.00
0.40
0.80
1.20
1.60
2.00
VELOCITY , (fps)

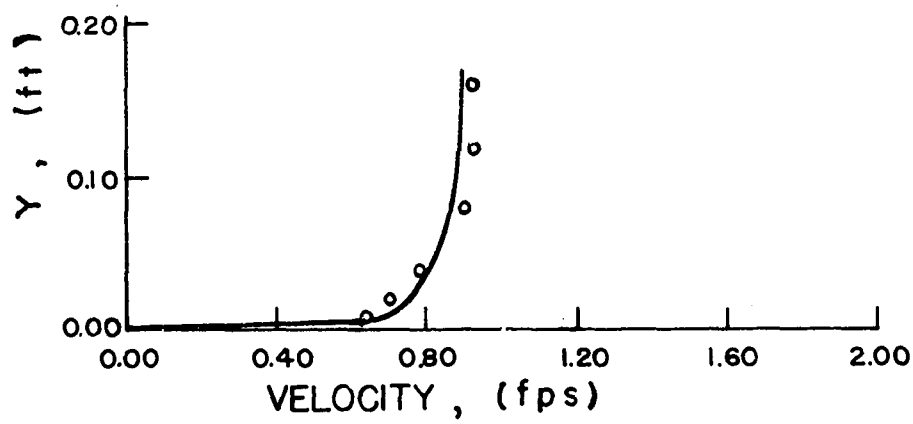
0.20
0.10
0.00
Y , (ft)
0.00
0.40
0.80
1.20
1.60
2.00
VELOCITY , (fps)

Equation of the curve: $v = 0.831 \left(\frac{y}{D}\right)^{0.154}$.

Fig. 21. Velocity profile curve. Y vs. velocity, where
Y = distance from bed in ft.
Tailgate setting 2 $\frac{5}{8}$ in. and depth of flow 0.122 ft.

Equation of the curve: $v = 0.694 \left(\frac{y}{D}\right)^{0.0471}$.

Fig. 22. Velocity profile curve. Y vs. velocity, where
Y = distance from bed in ft.
Tailgate setting 2 $\frac{4}{8}$ in. and depth of flow 0.107 ft.

Equation of the curve: $v = 0.691 \left(\frac{y}{D}\right)^{0.119}$.

Fig. 23. Velocity profile curve. Y vs. velocity, where
Y = distance from bed in ft.
Tailgate setting 2 $\frac{3}{8}$ in. and depth of flow 0.083 ft.

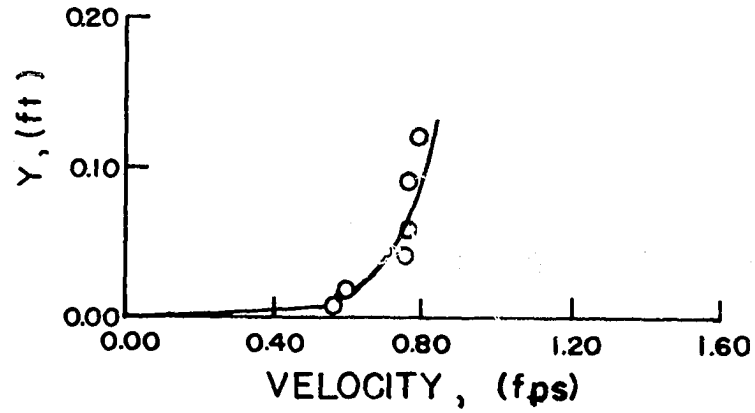
0.20
0.10
0.00
Y, (ft)
0.00
0.40
0.80
1.20
1.60
VELOCITY, (fps)

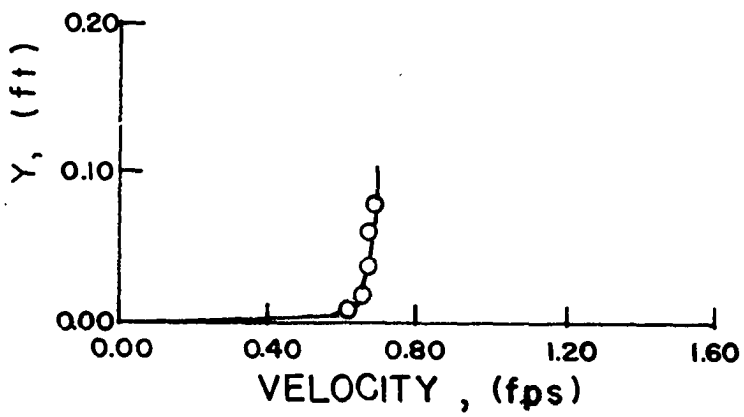
0.20
0.10
0.00
Y, (ft)
0.00
0.40
0.80
1.20
1.60
VELOCITY, (fps)

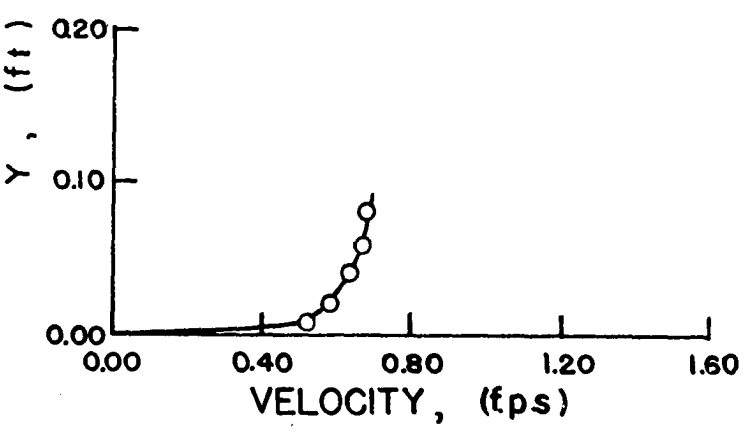
0.20
0.10
0.00
Y, (ft)
0.00
0.40
0.80
1.20
1.60
VELOCITY, (fps)

π_7 = 2,660 based on average centroidal velocity.

π_7 = 3,240-2,800 based on mean velocity.

Fig. 24. π_1 vs. π_3 using centroidal velocity and mean velocity.

π_7 = 2,500 based on average centroidal velocity.

π_7 = 2,970-2,570 based on mean velocity.

Fig. 25. π_1 vs. π_3 using centroidal velocity and mean velocity.

π_7 = 2,120 based on average centroidal velocity.

π_7 = 2,730-2,370 based on mean velocity.

Fig. 26. π_1 vs. π_3 using centroidal velocity and mean velocity.

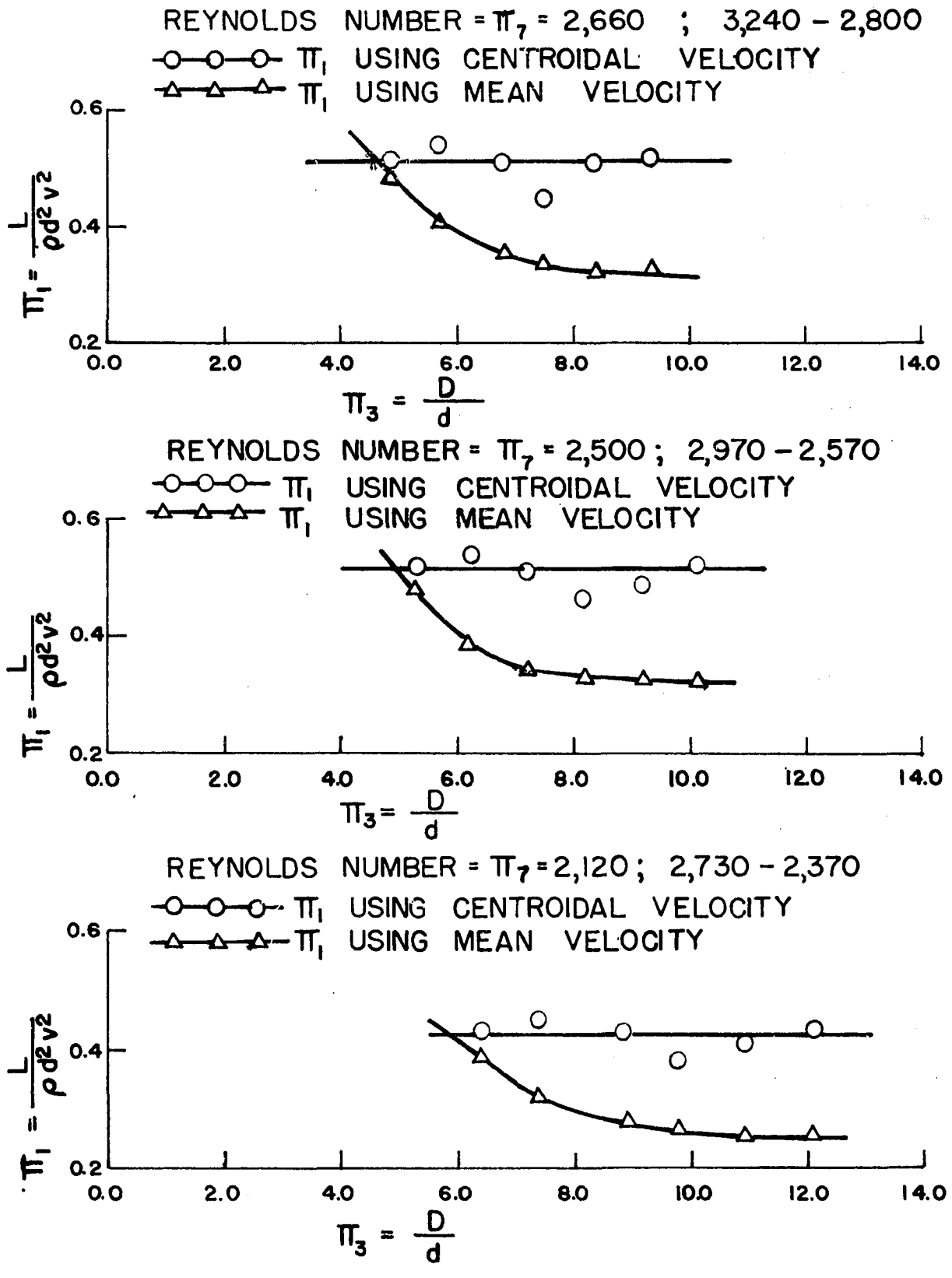
REYNOLDS NUMBER = π_7 = 2,660 ; 3,240 – 2,800
π_1 USING CENTROIDAL VELOCITY
π_1 USING MEAN VELOCITY
$\pi_1 = \frac{L}{\rho d^2 v^2}$
$\pi_3 = \frac{D}{d}$
0.6
0.4
0.2
0.0
2.0
4.0
6.0
8.0
10.0
12.0
14.0
REYNOLDS NUMBER = π_7 = 2,500 ; 2,970 – 2,570
π_1 USING CENTROIDAL VELOCITY
π_1 USING MEAN VELOCITY
$\pi_1 = \frac{L}{\rho d^2 v^2}$
$\pi_3 = \frac{D}{d}$
REYNOLDS NUMBER = π_7 = 2,120 ; 2,730 – 2,370
π_1 USING CENTROIDAL VELOCITY
π_1 USING MEAN VELOCITY
$\pi_1 = \frac{L}{\rho d^2 v^2}$
$\pi_3 = \frac{D}{d}$

π_7 = 1,730 based on average centroidal velocity.

π_7 = 2,240-1,940 based on mean velocity.

Fig. 27. π_1 vs. π_3 using centroidal velocity and mean velocity.

π_7 = 1,965 based on average centroidal velocity.

π_7 = 2,470-2,140 based on mean velocity.

Fig. 28. π_1 vs. π_3 using centroidal velocity and mean velocity.

π_7 = 1,590 based on average centroidal velocity.

π_7 = 1,940-1,545 based on mean velocity.

Fig. 29. π_1 vs. π_3 using centroidal velocity and mean velocity.

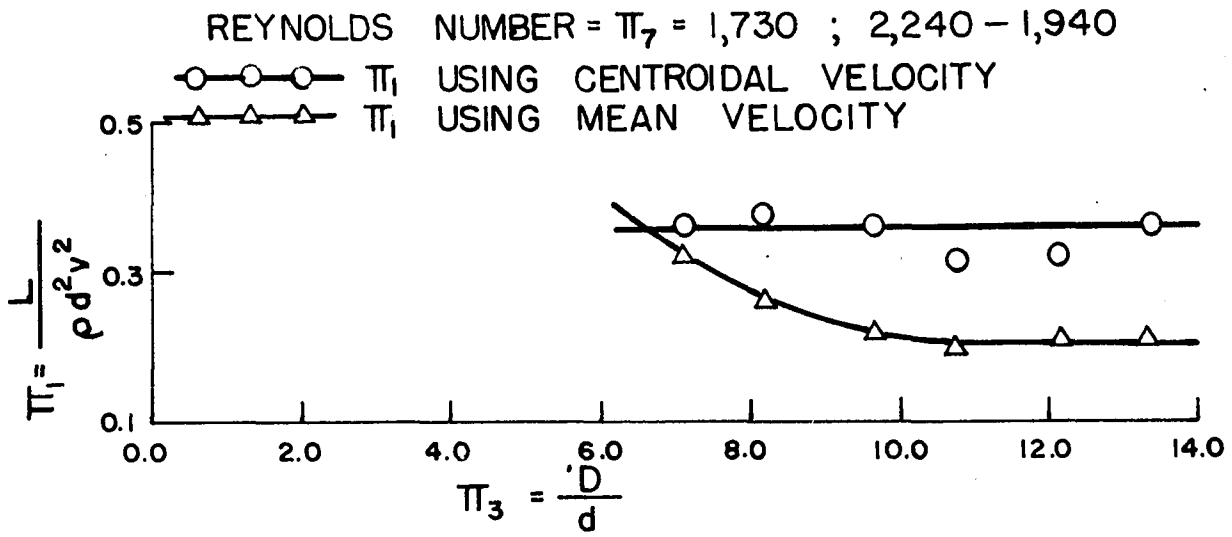
REYNOLDS NUMBER = π_7 = 1,730 ; 2,240 – 1,940
π_1 USING CENTROIDAL VELOCITY
π_1 USING MEAN VELOCITY
$\pi_1 = \frac{L}{\rho d^2 v^2}$
0.5
0.3
0.1
0.0
2.0
4.0
6.0
8.0
10.0
12.0
14.0
$\pi_3 = \frac{D}{d}$

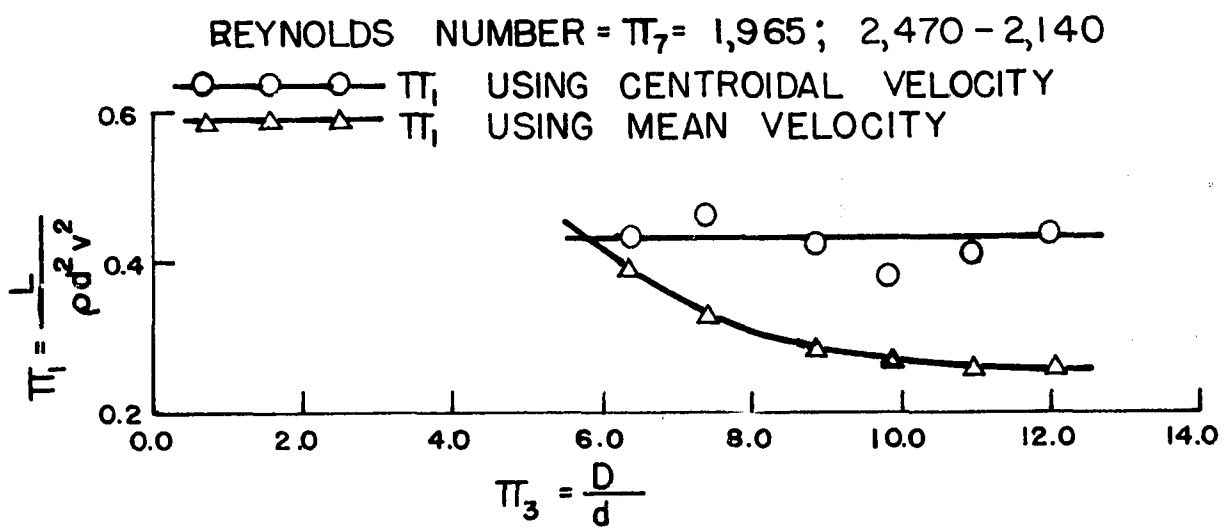
REYNOLDS NUMBER = π_7 = 1,965 ; 2,470 – 2,140
π_1 USING CENTROIDAL VELOCITY
π_1 USING MEAN VELOCITY
$\pi_1 = \frac{L}{\rho d^2 v^2}$
0.6
0.4
0.2
0.0
2.0
4.0
6.0
8.0
10.0
12.0
14.0
$\pi_3 = \frac{D}{d}$

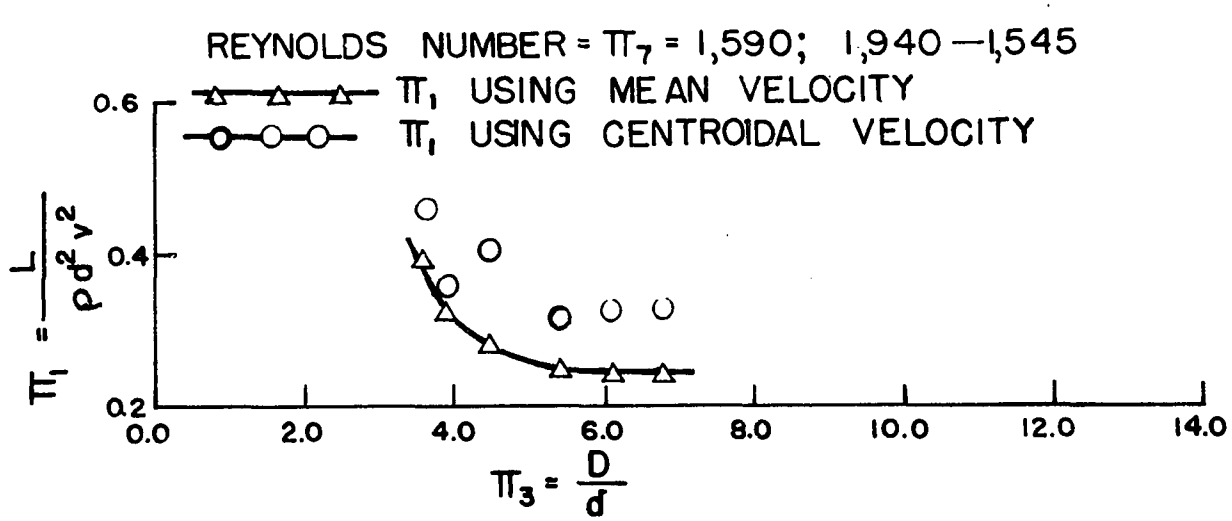
REYNOLDS NUMBER = π_7 = 1,590; 1,940 – 1,545
π_1 USING MEAN VELOCITY
π_1 USING CENTROIDAL VELOCITY
$\pi_1 = \frac{L}{\rho d^2 v^2}$
0.6
0.4
0.2
0.0
2.0
4.0
6.0
8.0
10.0
12.0
14.0
$\pi_3 = \frac{D}{d}$

investigation in the present study. The centroidal velocity is defined as that which occurs at the centroid of the area bounded by the velocity profile curve, the y-axis and the line y = d, where y = the distance from the bed of the channel and d = the diameter of the cylinder.

The mean velocity of flow in the channel for each set of critical conditions was determined from the corresponding velocity profile. The area bounded by the velocity profile curve, the y-axis and the line y = D, where D = the depth of flow in the channel, was divided by the depth of flow to obtain the mean velocity. See Appendix for calculations. The centroidal velocity was obtained by locating the centroid of the area bounded by the velocity profile curve, the y-axis and the line y = d. The velocity at this location was then determined by substituting the distance of the centroid from the bed of the channel into equation (15). See Appendix.

Two sets of Pi terms were calculated, one using the mean velocity and the other using the centroidal velocity. Hereafter the symbols v_m and v_c will be used to indicate the mean velocity and the centroidal velocity respectively. Each of the figures 24 to 34 shows two curves of π_1 versus π_3. One of the curves is based on π_1 and π_7 computed by using v_m, while the other is based on the Pi terms computed by using v_c. The two curves in each figure afford a comparison between the results obtained by using the mean velocity and the centroidal velocity.

π_7 = 1,451 based on average centroidal velocity.

π_7 = 1,780-1,420 based on mean velocity.

Fig. 30. π_1 vs. π_3 using centroidal velocity and mean velocity.

π_7 = 1,340 based on average centroidal velocity.

π_7 = 1,650-1,320 based on mean velocity.

Fig. 31. π_1 vs. π_3 using centroidal velocity and mean velocity.

π_7 = 1,185 based on average centroidal velocity.

π_7 = 1,480-1,180 based on mean velocity.

Fig. 32. π_1 vs. π_3 using centroidal velocity and mean velocity.

REYNOLDS NUMBER = π_7 = 1,451 ; 1,780 – 1,420

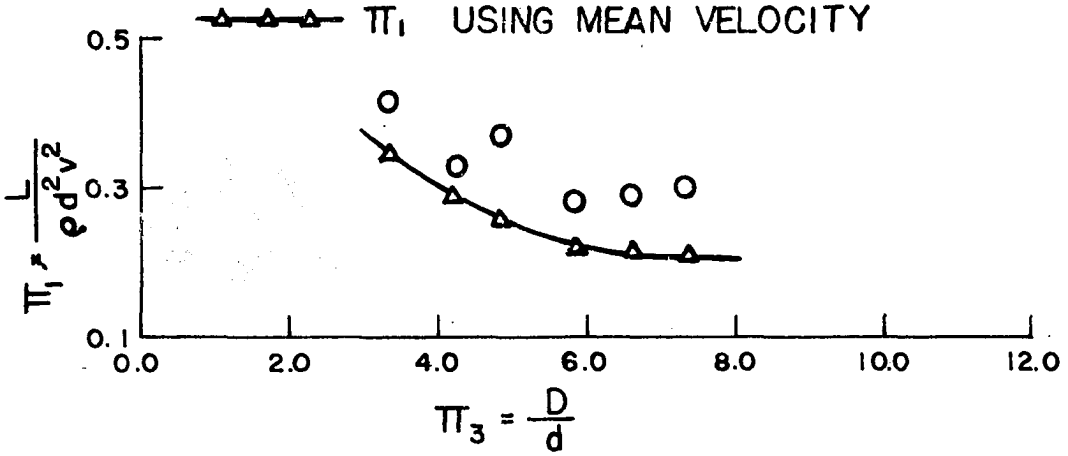

REYNOLDS NUMBER = π_7 = 1,340 ; 1,650 – 1,320

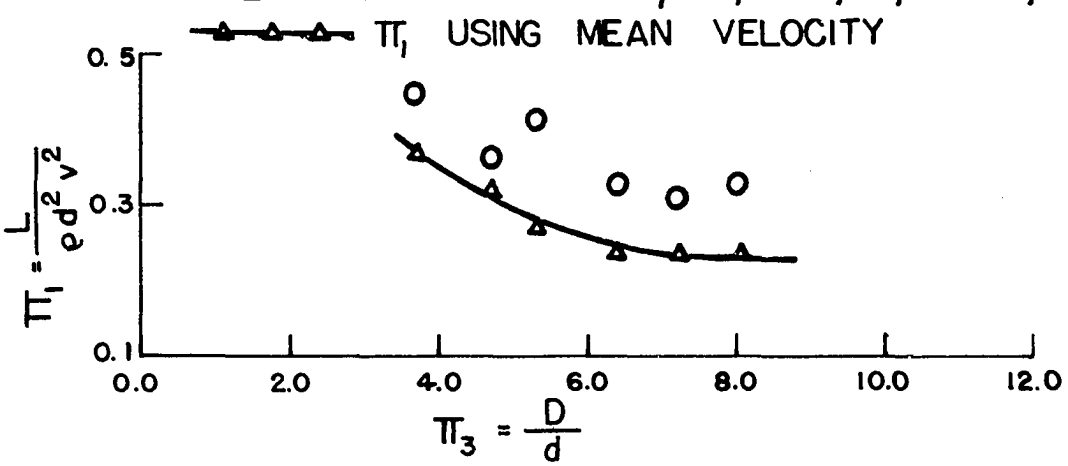

REYNOLDS NUMBER = π_7 = 1,185 ; 1,480 – 1,180

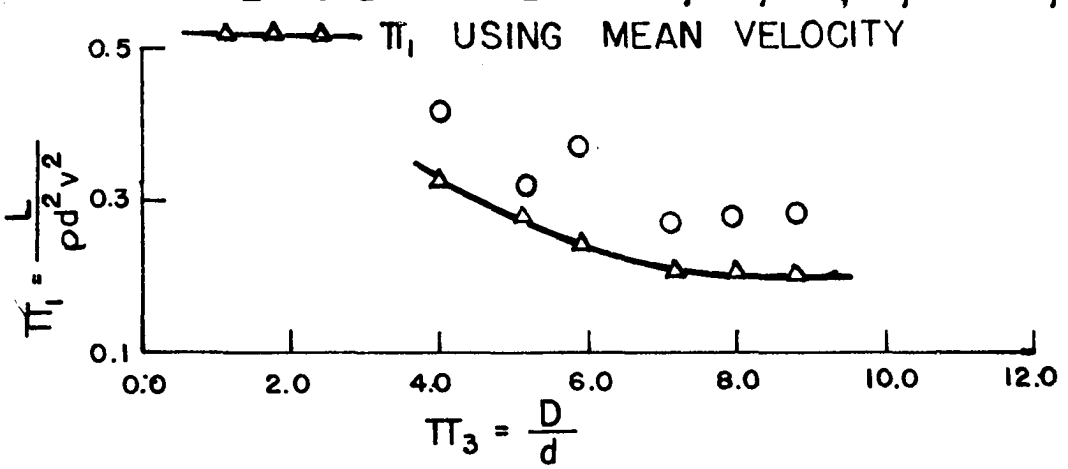

π_7 = 1,061 based on average centroidal velocity.

π_7 = 1,360-1,070 based on mean velocity.

Fig. 33. π_1 vs. π_3 using centroidal velocity and mean velocity.

π_7 = 935 based on average centroidal velocity.

π_7 = 1,190-950 based on mean velocity.

Fig. 34. π_1 vs. π_3 using centroidal velocity and mean velocity.

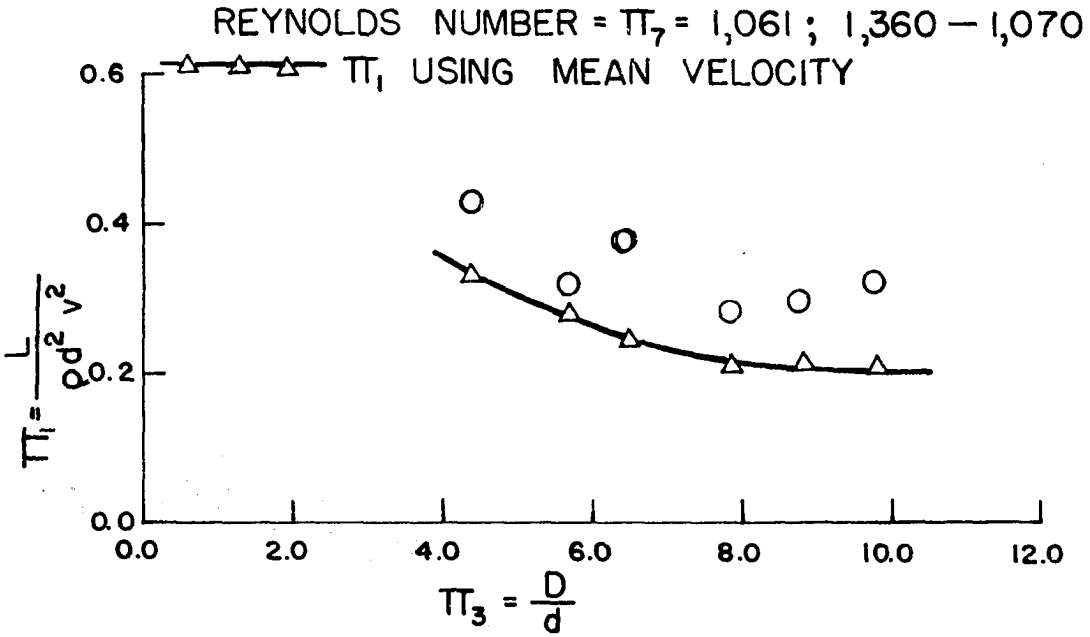
REYNOLDS NUMBER = π_7 = 1,061 ; 1,360 — 1,070
π_1 USING MEAN VELOCITY
0.6
0.4
0.2
0.0
$\pi_1 = \frac{L}{\rho d^2 v^2}$
0.0
2.0
4.0
6.0
8.0
10.0
12.0
$\pi_3 = \frac{D}{d}$

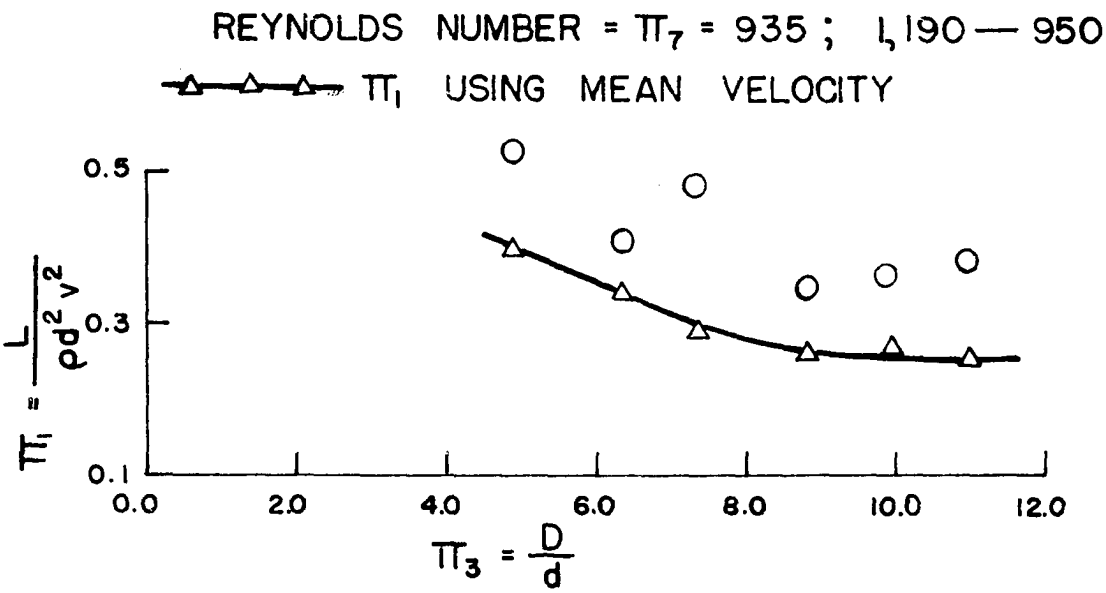
REYNOLDS NUMBER = π_7 = 935 ; 1,190 — 950
π_1 USING MEAN VELOCITY
0.5
0.3
0.1
$\pi_1 = \frac{L}{\rho d^2 v^2}$
0.0
2.0
4.0
6.0
8.0
10.0
12.0
$\pi_3 = \frac{D}{d}$

The data from which each graph was plotted were obtained for a given cylinder tested for six different tailgate settings. Thus the diameter was kept constant while the depth of flow was varied. The Reynolds number indicated in each figure was computed using the average value of v_c. The range of Reynolds number when v_m was used for the computation is also noted on each figure.

The curves obtained by plotting π_1 against π_3, when the Pi terms are computed by using v_m, indicate that π_1 is dependent on π_3 when the other Pi terms remain constant. There is a slight variation in the Reynolds number whose effect has been disregarded. On the other hand, for the curves in which π_1 and π_7 were computed by using v_c the dependency of π_1 on π_3 is not so evident. In fact, the curves in figures 24 to 28 seem to indicate that for the range of the present investigation π_1 is independent of π_3. The scatter of points when π_1 is plotted against π_3 when the Pi terms are computed by using v_c is discussed later.

If π_1 is independent of π_3 when v_c is used as the significant velocity, as the curves seem to indicate, then the depth of flow may be eliminated from the list of variables influencing lift. For in π_3, that is $\frac{D}{d}$, d is kept constant and only D is varied. It should be emphasized that only the curves of figures 24 to 28 seem to indicate that π_1 may be independent of π_3, those from figures 29 to 34 show wide scatter of points and neither set of curves yield conclusive

evidence that π_1 is independent of π_3 when v_c is used as significant velocity.

Variation of π_1 with π_7

Table 1 shows the variation of π_1 with π_7 assuming that v_c is the significant velocity. The average value of v_c for a given cylinder and the different tailgate settings were used in computing π_1 and π_7. These data are plotted on rectangular coordinates in Fig. 35. The resulting curve seems to indicate that a functional relationship exists between π_1 and π_7. The range of Reynolds number in the present investigation is too narrow to develope the actual functional relationship. Fig. 36 shows π_1 plotted against π_7 using v_m as the significant velocity, the value of π_3 varying between 6.17 and 6.81. The scatter of points on this graph is too wide to justify drawing a curve. Data for plotting the graph are given in Table 7, Appendix.

π_1 as shown in Table 1 and plotted in Fig. 32 may be considered as a lift coefficient. That is,

$$\frac{L}{\rho v^2 d^2} = C_L$$

where C_L = the lift coefficient which lies between 0.507 and 0.327 for the present investigation.

Table 1. Variation of π_1 with π_7 for the range of the investigation[a]

π_1 $\frac{L}{\rho d^2 v_c^2}$	π_7 $\frac{\rho v_c d}{\mu}$
0.507	2660
0.507	2500
0.428	2120
0.428	1965
0.355	1730
0.365	1590
0.333	1450
0.365	1340
0.327	1185
0.340	1061
0.419	935

[a] L = lift,
d = diameter of cylinder,
v_c = average centroidal velocity used as significant velocity,
ρ = density of fluid,
μ = viscosity of fluid.

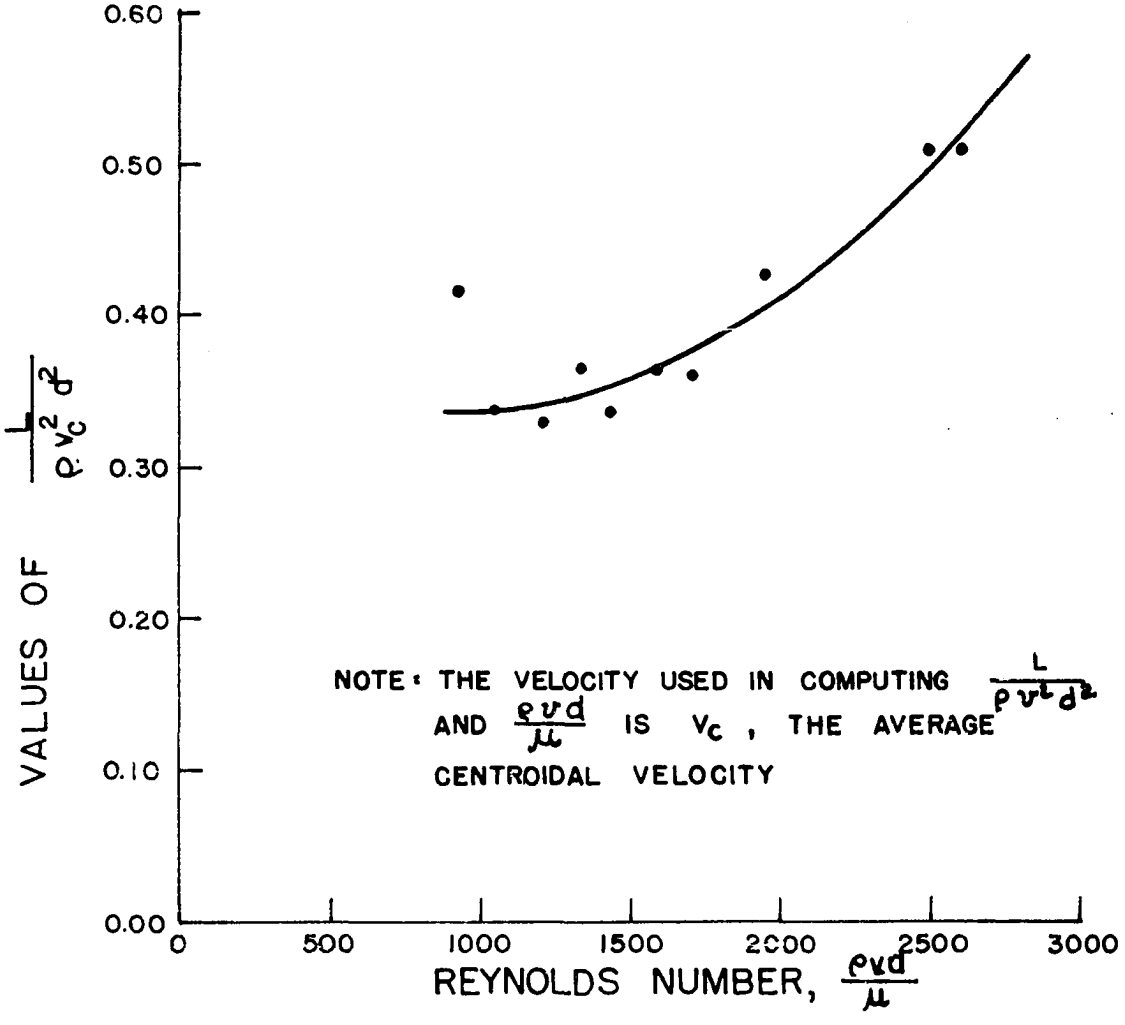

Fig. 35. π_1 vs. π_7 .

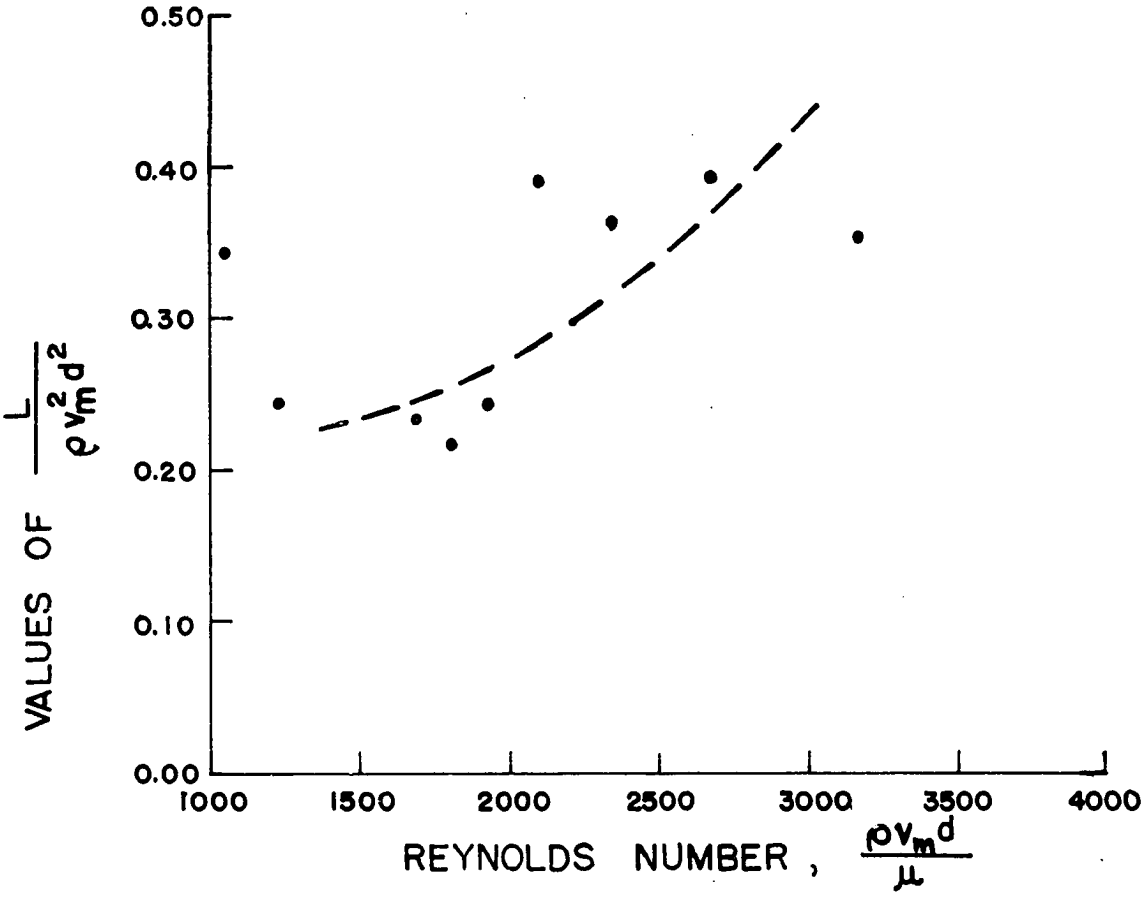

Fig. 36. π_1 vs. π_7, π_3 having values between 6.17 and 6.81.

Comparison between Experimental and Theoretical Lift

The theoretical lift at incipient motion as determined in equation (11) is

$$L = \pi \rho a U^2 \left[\frac{1}{3} + \frac{\pi^2}{9} \right] . \qquad (16)$$

The lift given in equation (16) is for a unit length of a cylinder. The values of L_{v_m} shown in Table 2 were determined by substituting v_m for U in equation (16). For a given tailgate setting v_m is constant. The v_m used for computing L_{v_m} given in Table 2 was that corresponding to the three-inch tailgate setting. The values of L_{v_c} shown in Table 2 were determined by substituting v_c for U in equation (16). v_m and v_c stand for the mean and centroidal velocities respectively at incipient motion of cylinders.

The value of L_{ob} shown in the table are those for lift computed from the observed data. There is little agreement between the theoretical lift and the observed lift, whether v_m or v_c is used for computations.

Table 2. Comparison between lift obtained experimentally and lift obtained from potential theory[a]

a (in.)	l (in.)	γ	v_m fps	v_c fps	L_{v_m} 10^{-4} lb.	L_{v_c} 10^{-4} lb.	L_{ob} 10^{-4} lb.
0.162	1.297	1.20	1.292	1.055	215	141	7.86
0.150	1.202	1.20	1.292	1.042	182	118	6.55
0.138	1.101	1.20	1.292	1.035	152	97.5	5.10
0.125	1.002	1.20	1.292	1.024	126	79.5	3.66
0.113	0.903	1.20	1.292	1.019	103	64.2	2.45
0.162	1.301	1.05	0.775	0.652	77.5	54.5	2.07
0.150	1.203	1.05	0.775	0.645	65.8	45.2	1.59
0.138	1.097	1.05	0.775	0.640	54.8	36.8	1.43
0.125	1.001	1.05	0.775	0.634	45.4	30.5	1.03
0.113	0.903	1.05	0.775	0.628	37.1	24.5	0.861
0.100	0.801	1.05	0.775	0.607	35.5	21.8	0.817

[a] a = radius of cylinder,
l = length of cylinder,
γ = average specific gravity of the material of the cylinder,
L_{v_m} = lift computed from the expression $\pi \rho a U^2 (\frac{1}{3} + \frac{1}{9}\pi^2)$/unit length using v_m for U,
L_{v_c} = lift computed from the expression $\pi \rho a U^2 (\frac{1}{3} + \frac{1}{9}\pi^2)$/unit length using v_c for U,
L_{ob} = lift observed in the present investigation.

DISCUSSION

Incipient Motion of Cylinders

The incipient motion of each cylinder was considered to be that corresponding to the first observable bouncing of the cylinder against the bed of the channel. The lift at incipient motion was then taken to be equal to the weight of the cylinder in water. This would be true only in case the acceleration in the vertical direction is zero. Since a cylinder is originally at rest it must accelerate in order to move in any direction. Therefore, when it is bouncing on the bed of the channel it must possess acceleration in a vertical direction. Consequently, the forces in the vertical direction will not balance and the lift will exceed the bouyant weight of the cylinder by the inertia force on the cylinder at incipient motion.

An attempt was made to estimate the error involved in disregarding the effect of acceleration in the determination of lift. Observations were made on the 0.325 in. diameter cured polyester resin cylinder at critical conditions. It was estimated that the amplitude of the bouncing of the cylinder was 0.06 in. and the frequency, 1 cycle per second. The motion of the cylinder was assumed to be simple harmonic. From the amplitude and the frequency of motion of the cylinder its acceleration was computed. The product of the acceleration and the mass of the cylinder gave the inertia force. The inertia force thus estimated was found to be about three

percent of the bouyant weight of the cylinder. For the remaining cylinders, the percent of error involved would be still less. Thus the assumption that incipient upward motion of a cylinder corresponds to its first observable bouncing on the bed of the channel appears to be reasonable.

Five cylinders of one material having a specific gravity of 1.20 and six cylinders of another having a specific gravity of 1.05 were tested. Each cylinder was tested for six different tailgate settings. Thus the combination of cylinders and tailgate settings should have resulted in 66 (that is, 11 times 6) different flow conditions for incipient motion of the cylinders. However, for all the cylinders of one material the flow conditions coincided (Table 4, Appendix). That is, for a given tailgate setting the conditions for incipient motion for all the cylinders of one material were the same. This apparently strange result can be explained from the point of view of significant velocity.

When v_m was considered as the significant velocity, π_1 was found to be dependent on π_3, when the other Pi terms remained constant. The small variation in Reynolds number is disregarded. (Refer to Fig. 24 to 34.) Thus,

$$\frac{L}{\rho v_m^2 d^2} = f\left(\frac{D}{d}\right) \quad . \tag{17}$$

For a given tailgate setting the depth of flow D is constant. The diameter d changes from cylinder to cylinder. Therefore,

$f(\frac{D}{d})$ is not a constant.

Lift as determined in the present investigation is taken to be equal to the bouyant weight of the cylinder. That is,

$$L = \frac{\pi}{4} d^2 l(\rho_1 - \rho)g \qquad (18)$$

where

d = diameter of the cylinder,

l = length of the cylinder,

ρ_1 = density of the material of the cylinder,

ρ = density of water and

g = acceleration due to gravity.

Substituting this value of L in equation (17) and dividing both sides by $v_m^2 d^2$,

$$\frac{L}{\rho v_m^2 d^2} = \frac{\frac{\pi}{4} d^2 l(\rho_1 - \rho)g}{\rho v_m^2 d^2} = \frac{\frac{\pi}{4}(\frac{\rho_1}{\rho} - 1) gl}{v_m^2} .$$

For a given material $\frac{\pi}{4}(\frac{\rho_1}{\rho} - 1)$ is a constant. Indicating this by C_1

$$\frac{\frac{\pi}{4}(\frac{\rho_1}{\rho} - 1) gl}{v_m^2} = C_1 \frac{l}{v_m^2} .$$

For a given tailgate setting and depth of flow v_m is the same. Thus

$$C_1 \frac{l}{v_m^2} = C_2 l \qquad (19)$$

where $C_2 = \frac{C_1}{v_m^2}$.

From equations (17) and (19),

$$C_2 l = f(\frac{D}{d}) = f(\frac{k}{d})$$

where k = D = a constant. This may be rewritten as $l = f_3(\frac{l}{d})$ which is valid since the ratio of l to d was kept constant for the present investigation. From this it may be concluded that the mean velocity may be used as the significant velocity provided the depth of flow is also included as a pertinent variable.

When the Pi terms were computed considering v_c as the significant velocity, the curves of π_1 vs. π_3 (Fig. 24 to 34) appeared to indicate that π_1 could be independent of π_3. The data obtained in the present investigation do not conclusively prove this to be the case. Nevertheless, the observation under discussion deserves examination on the assumption that π_1 is independent of π_3 when the other Pi terms remain constant. When v_c is considered as the velocity significant in the phenomenon of lift, the depth of flow may be eliminated from the list of variables affecting lift. Under this premise, for the observation stated above, π_1 becomes a constant. That is,

$$\frac{L}{\rho v_c^2 d^2} = k_1 = \text{a constant.}$$

Substituting for L the value shown in equation (18) and simplifying in the same manner as before,

$$\frac{L}{\rho v_c^2 d^2} = k_2 \frac{l}{v_c^2}$$

or

$$\frac{L}{v_c^2} = k_3 = \text{a constant.}$$

This result is quite reasonable. A constant ratio of l to d was kept for the present investigation. Thus a change in l results in a corresponding change in d. For a given tailgate setting and depth of flow a change in d results in a change in the location of the centroid and thus a change in the value of v_c. In other words, as l increases v_c also increases. Consequently, the ratio of l to d could well remain a constant. It may be mentioned here that the observation of the same flow conditions for a given tailgate setting for all of the cylinders of one material led to the trial of v_c as the significant velocity.

As stated earlier, the curves of π_1 plotted against π_3 using v_c as the significant velocity (Fig. 24 to 34) do not conclusively prove that π_1 is independent of π_3, when the other Pi terms remain constant. The data plotted in Fig. 29 to 34 show too wide a scatter to justify the drawing of any curves. Fig. 29 to 34 correspond to tests on cylinders made of the material having a specific gravity of 1.05. The bouncing of these cylinders was slow and erratic, and it was difficult to match exactly the type of bouncing from cylinder to cylinder.

This may be a possible reason for the large scatter of points.

Figures 24 to 28 are drawn from data obtained from tests on cylinders made of the material having a specific gravity of 1.20. The bouncing of these cylinders was fairly rapid, the estimated frequency being one cycle per second, and it was comparatively easy to match similar types of bouncing from cylinder to cylinder. These figures seem to indicate the possibility of the centroidal velocity being significant. In these figures it appears that a curve of sinusoidal shape would fit the data better than a straight line. However, if the value of π_1 for the fourth point from left were slightly greater, a straight line would have been the appropriate fit. It is probable that the low value of π_1 for the fourth point resulted from experimental error.

Each of the figures 24 to 34 shows the data obtained from one cylinder and six different tailgate settings. Since, for all the cylinders in one material the critical conditions of flow coincided for each tailgate setting, in this set of figures, one is different from the other only because of the use of different cylinders. Thus the curves in figures 24 to 28 are similar in shape. Also the manner in which the points are scattered in figures 29 to 34 tends to be the same.

Depth of Flow and Significant Velocity

The velocity of flow that would affect the lift on a cylinder resting on the bed of a channel is some velocity in

the vicinity of the cylinder. The identification of this velocity, termed the significant velocity in this thesis, is very important in the understanding of the phenomenon of lift. When this velocity is not known, it could be replaced by other variables that would define it. Thus when depth of flow and mean velocity are considered pertinent to lift, together they define the single variable, the significant velocity. In other words, the mean velocity and the depth of flow when used together effectively conceal the fact of the significant velocity. When the significant velocity is identified, it could replace the mean velocity and the depth of flow from the list of variables affecting lift. This would not only reduce the number of variables involved but would also be a big step in the understanding of lift.

Experimental Determination of Lift

The technique used in the present investigation to determine lift is simple and direct. The interference with the flow conditions is reduced to a minimum. The slight obstruction to the flow caused by the needles which are inserted into the bed of the channel 18 inches upstream from the cylinder would have no effect on the flow conditions in the vicinity of the cylinder. The threads, which are parallel to the bed of the channel and which are placed in a region of the channel where the flow is uniform, will have little influence on the movement of the cylinder in a vertical direction

at incipient motion.

The Pi term containing lift, the dependent variable, is π_1. Table 1 gives the variation of π_1 and π_7, the Reynolds number. v_c is used in the computation of the Pi terms. The data in Table 1 are plotted in Fig. 35. The latter shows that a functional relationship exists between the two Pi terms. In order to develop this functional relationship the data were plotted on a logarithmic chart. As the range of Reynolds number under which the present investigation was carried out was narrow, such a plot resulted in nothing more than a cluster of points in a small region of the graph. Since such a graph has no significance it has been omitted from this thesis.

Fig. 36 shows π_1 plotted against π_7, for a value of π_3 equal to 6.00-6.99, this time v_m being used for computations. The scatter of the points in this graph is too great to justify the drawing of any curves. For the same reason similar graphs of π_1 plotted against π_7 for other values of π_3 are omitted from this thesis.

The lift coefficient is usually defined by the following relationship

$$L = C_L \rho A \frac{v^2}{2}$$

where A = a significant area and C_L = the lift coefficient. Viewed in this light π_1 as shown in Table 1 and plotted in Fig. 35 may be considered as a form of lift coefficient.

This may be shown as follows:

$$\frac{L}{\rho v^2 d^2} = C_L \qquad (20)$$

where C_L = lift coefficient which lies between 0.507 and 0.327. This may be rewritten as

$$L = C_L \rho v^2 d^2$$

$$= C_L \rho A v^2 \frac{d}{l}$$

where $A = dl$, the projected area of the cylinder.

This is

$$= \frac{1}{2} C_L \rho A \frac{v^2}{2}$$

since $\frac{d}{l} = \frac{1}{4}$ for the present investigation.

Theoretical Lift

Table 2 shows two sets of values for theoretical lift, one set calculated by using v_m and the other by using v_c, v_m and v_c being the observed mean and centroidal velocities respectively at incipient motion. The theoretical lift thus calculated is about 20 to 30 times more than what was observed experimentally at incipient motion.

The most important reason for this lack of agreement between the two values is that the theoretical expression is derived on the basis of idealized conditions. It does not take into account viscosity, and thus disregards the velocity

variation in the vertical direction in the undisturbed flow. Irrotational flow is assumed so that the potential theory could be applied. According to potential theory, the section of the cylinder by a plane parallel to the flow is a stream line. In other words, the separation of the flow from the cylinder which is actually observed is disregarded. This could result in serious error in the determination of forces acting on the cylinder. The effects of surface roughness of the cylinder and that of the channel are also disregarded in the derivation of the theoretical expression.

SUMMARY AND CONCLUSIONS

The phenomenon of incipient upward motion of a circular cylinder resting on the bed of a channel with its axis perpendicular to the flow was chosen for investigation. Only two dimensional flow was considered. The problem was approached from the point of view of dimensional analysis. Ten variables were considered pertinent. Using the Buckingham Pi theorem, these variables were rewritten as seven dimensionless groups of variables.

Eleven different cylinders made of two different materials were tested for incipient motion in an open channel. Each cylinder was held in position for testing by two cotton threads which were tied at one end to the cylinder and at the other end to two needles. The needles were inserted into the bed of the channel so that the threads remained parallel to each other and to the bed of the channel.

At incipient motion of each cylinder, which was considered to correspond to a pronounced bouncing of the cylinder, the conditions of flow were noted. The lift was considered as the weight of the cylinder in water. It was determined by weighing the cylinder in water, the liquid that was used for the investigation.

The velocity profile corresponding to the conditions of flow for each case of incipient motion was determined and the results plotted. A micromanometer with a gage fluid of carbon tetrachloride and attached to a small pitot was used for the

velocity determination.

An attempt was made to establish the significant velocity that influences the lift. Two different velocities were considered, one the mean velocity of flow in the channel and the other, the velocity at the centroid of the area bounded by the velocity profile curve, the Y-axis and the line y = d, where d = the diameter of the cylinder.

There were some indications that for the range in which the present investigation was conducted, the centroidal velocity might be the significant velocity that influenced lift.

The observed lift was compared with the lift computed on the basis of an expression developed by Harold Jeffreys (3) using potential theory. The theoretical lift corresponding to the observed velocity at which incipient motion took place was found to be several times larger than the observed lift.

It was concluded that lift could be determined by the technique used in the present investigation.

SUGGESTIONS FOR FURTHER STUDY

The present study was conducted within a narrow range of Reynolds Numbers. It is recommended that the range be extended. This may be done by varying the diameter and material of the cylinders and by using liquids other than water.

It is recommended that studies be conducted to determine the influence of the length of the cylinder, the roughness of the channel bed, the surface roughness of the cylinders and the slope of the channel on the lift.

An analytical solution for the lift experienced by a cylinder in two dimensional flow assuming a straight line variation for the velocity profile has been given by Hsue-Shen Tsien (10). It is recommended that an attempt be made to find a similar solution for the case when the velocity profile is of the type developed in this thesis.

LITERATURE CITED

1. Einstein, A.H. and El-Sayed Ahmed El-Samni. Hydrodynamic forces on a rough wall. Rev. of Mod. Phys. 21: 520-524, 1949.

2. Encyclopaedia Britannica. Soil erosion. Vol. 20. 934C. Chicago, Encyclopaedia Britannica Inc. 1957.

3. Jeffreys, Harold. On the transport of sediments by stream. Proc. Camb. Phil. Soc. 25: 272-276, 1929.

4. Lacey, G. Stable channels in alluvium. Min. Proc. Inst. Civ. Eng. 229: 259-270, 1930.

5. Leliavsky, S. An introduction to fluvial hydraulics. London, Constable and Company, Ltd. 1955.

6. Matthes, G.H. On sand movements in fluvial models. Trans. Am. Soc. Civ. Eng. 61: 844, 1935.

7. Murphy, Glenn. Similitude in engineering. New York, The Ronald Press Company. 1950.

8. _____ Mechanics of fluids. 2nd. ed. Scranton, Penn, International Text Book Company. 1952.

9. Rubey, W.W. The force required to move particles on a stream bed. Professional Paper 189-E of U.S. Dept. of Int., 1938.

10. Tsien, Hsue-Shen. Symmetrical Joukosky airfoils in shear flow. Quart. Ap. Math. 1: 130-138, 1943.

11. Vanoni, V.A. A summary of sediment transportation mechanics. Fluid Mechanics Conf. Proc. 3: 129-156, 1953.

12. White, C.M. The equilibrium of grains on the bed of a stream. Proc. Roy. Soc. Lond. Series a, 174: 323-324, 1940.

13. Young, D.F. Drag and lift on spheres within cylindrical tubes. To be published in Journal of the Hydraulic Division, Am. Soc. Civ. Eng., [ca. 1960]

ACKNOWLEDGMENTS

The author is grateful to Dr. Glenn Murphy, Head of the Department of Theoretical and Applied Mechanics, for his guidance and helpful criticisms. The author gratefully acknowledges the help and suggestions given by Dr. D. F. Young, Professor of Theoretical and Applied Mechanics, throughout the period of investigation and the preparation of the thesis. The encouragement given by Professor Hobart Beresford, Head of the Department of Agricultural Engineering, is gratefully appreciated. Thanks are also due to Dr. H. P. Johnson, Professor of Agricultural Engineering for his encouragement and valuable advice.

APPENDIX

Table 3. Determination of the properties of cylinders

No.	Diam. in. (d)	Length in. (l)	Wt. in air gm. (W_1)	Wt. in water gm. (W_2)	Lift (10^{-4}) lb.	W_1-W_2 gm.	Sp.gr. (γ)	Av. (γ)
Material: Cured polyester resin								
1	0.325	1.30	2.083	0.357	7.86	1.726	1.21	
2	0.300	1.20	1.721	0.297	6.55	1.424	1.21	
3	0.276	1.10	1.333	0.231	5.10	1.102	1.21	
4	0.250	1.00	1.009	0.166	3.66	0.843	1.20	
5	0.226	0.90	0.726	0.111	2.45	0.615	1.18	1.20
Material: Plastic								
1	0.325	1.30	2.043	0.094	2.07	1.949	1.05	
2	0.300	1.20	1.651	0.072	1.59	1.579	1.05	
3	0.276	1.10	1.272	0.065	1.43	1.207	1.05	
4	0.250	1.00	1.014	0.047	1.03	0.967	1.05	
5	0.226	0.90	0.795	0.039	0.861	0.756	1.05	
6	0.201	0.80	0.601	0.037	0.817	0.564	1.06	1.05

Table 4. Data for incipient motion of cylinders

Diam. in. (d)	Length in. (l)	Point gage ft. bed	Point gage ft. water surface	Tailgate setting* in.	Manometer in. left	Manometer in. right	Temp. °C	Sp.gr. of cylinder
0.276	1.100	1.506	1.757	3	-2.35	-1.50	21.0	1.20
			1.758		-2.35	-1.50		
			1.758		-2.35	-1.50		
			1.758		-2.35	-1.50		
0.276	1.100	1.506	1.734	2 7/8	-1.90	-1.10	21.0	1.20
			1.733		-1.90	-1.10		
			1.734		-1.90	-1.10		
			1.735		-1.90	-1.10		
0.276	1.100	1.506	1.708	2 6/8	-1.50	-0.65	21.0	1.20
			1.710		-1.60	-0.75		
			1.709		-1.55	-0.70		
			1.709		-1.55	-0.70		
0.276	1.100	1.506	1.685	2 5/8	-1.25	-0.30	21.5	1.20
			1.692		-1.40	-0.45	21.5	
			1.691		-1.40	-0.45	22.0	
			1.692		-1.40	-0.45	22.0	
0.276	1.100	1.506	1.659	2 4/8	-1.00	-0.05	22.0	1.20
			1.658		-1.00	-0.05		
			1.662		-1.05	-0.10		
			1.660		-1.05	-0.10		
0.276	1.100	1.506	1.640	2 3/8	-0.95	0.00	22.5	1.20
			1.637		-0.95	0.00		
			1.638		-0.95	0.00		
			1.639		-0.95	0.00		
0.325	1.30	1.506	1.750	3	-2.35	-1.45	24.0	1.20
			1.751		-2.35	-1.45		
			1.752		-2.35	-1.45		
			1.757		-2.40	-1.50		
0.325	1.30	1.506	1.734	2 7/8	-1.95	-1.10	23.5	1.20
			1.734		-1.95	-1.10		
			1.735		-1.95	-1.10		
			1.733		-1.95	-1.10		

*The height of tailgate setting is considered from a fixed datum which is lower than the bed of the channel.

Table 4 (Continued)

Diam. in. (d)	Length in. (l)	Point gage ft. bed	Point gage ft. water surface	Tailgate setting in.	Manometer in. left	Manometer in. right	Temp. ^{o}C	Sp.gr. of cylinder
0.325	1.30	1.506	1.710	2 6/8	-1.60	-0.70	22.0	1.20
			1.707		-1.50	-0.60		
			1.709		-1.60	-0.70		
			1.710		-1.60	-0.70		
0.325	1.30	1.506	1.689	2 5/8	-1.35	-0.40	22.5	1.20
			1.689		-1.35	-0.40		
			1.690		-1.35	-0.40		
			1.690		-1.35	-0.40		
0.325	1.30	1.506	1.658	2 4/8	-0.95	0.00	23.0	1.20
			1.661		-1.00	-0.05		
			1.660		-1.00	-0.05		
			1.661		-1.00	-0.05		
0.325	1.30	1.506	1.638	2 3/8	-0.90	-0.05	23.0	1.20
			1.643		-0.95	0.00		
			1.639		-0.90	-0.05		
			1.640		-0.95	0.00		
0.300	1.20	1.506	1.679	2 5/8	-1.30	-0.35	21.0	1.20
			1.686		-1.40	-0.45		
			1.687		-1.40	-0.45		
			1.688		-1.45	-0.50		
0.300	1.20	1.506	1.653	2 4/8	-1.05	-0.10	21.5	1.20
			1.658		-1.10	-0.15		
			1.659		-1.10	-0.15		
			1.660		-1.15	-0.20		
0.300	1.20	1.506	1.638	2 3/8	-0.95	-0.00	21.5	1.20
			1.640		-0.95	-0.00		
			1.641		-0.90	-0.05		
			1.641		-0.90	-0.05		
0.250	1.00	1.506	1.682	2 5/8	-1.35	-0.40	22.0	1.20
			1.687		-1.40	-0.45		
			1.685		-1.40	-0.45		
			1.686		-1.40	-0.45		

Table 4 (Continued)

Diam. in. (d)	Length in. (l)	Point gage ft. bed	Point gage ft. water surface	Tailgate setting in.	Manometer in. left	Manometer in. right	Temp. °C	Sp.gr. of cylinder
0.225	0.90	1.506	1.672	2 5/8	-1.30	-0.30	22.0	1.20
			1.677		-1.30	-0.30		
			1.678		-1.35	-0.35		
			1.676		-1.45	-0.50		
0.276	1.10	1.505	1.690	3	-0.90	-0.00	23.0	1.05
			1.689		-0.90	-0.00		
			1.688		-0.90	-0.00		
			1.689		-0.90	-0.00		
0.276	1.10	1.505	1.670	2 7/8	-0.80	-0.10	23.0	1.05
			1.672		-0.80	-0.10		
			1.670		-0.80	-0.10		
			1.669		-0.80	-0.10		
0.276	1.10	1.505	1.652	2 6/8	-0.70	-0.20	23.0	1.05
			1.650		-0.70	-0.20		
			1.653		-0.70	-0.20		
			1.654		-0.70	-0.20		
0.276	1.10	1.505	1.630	2 5/8	-0.65	-0.25	23.0	1.05
			1.628		-0.65	-0.25		
			1.627		-0.65	-0.25		
			1.629		-0.65	-0.25		
0.276	1.10	1.505	1.611	2 4/8	-0.55	-0.30	23.0	1.05
			1.611		-0.55	-0.30		
			1.614		-0.55	-0.30		
			1.612		-0.55	-0.30		
0.276	1.10	1.505	1.588	2 3/8	-0.55	-0.30	23.0	1.05
			1.587		-0.55	-0.30		
			1.588		-0.50	-0.35		
			1.590		-0.50	-0.35		
0.325	1.30	1.506	1.629	2 5/8	-0.60	-0.25	22.0	1.05
			1.630		-0.60	-0.25		
			1.628		-0.60	-0.25		
			1.631		-0.60	-0.25		

Table 4 (Continued)

Diam. in. (d)	Length in. (l)	Point gage ft. bed	Point gage ft. water surface	Tailgate setting in.	Manometer in. left	Manometer in. right	Temp. °C	Sp.gr. of cylinder
0.300	1.20	1.506	1.627	2 5/8	-0.60	-0.25	22.0	1.05
			1.625		-0.55	-0.30		
			1.630		-0.60	-0.25		
			1.628		-0.60	-0.25		
0.250	1.00	1.506	1.625	2 5/8	-0.55	-0.30	22.0	1.05
			1.627		-0.60	-0.25		
			1.626		-0.55	-0.30		
			1.628		-0.60	-0.25		
0.225	0.90	1.506	1.628	2 5/8	-0.60	-0.25	22.5	1.05
			1.626		-0.60	-0.25		
			1.629		-0.60	-0.25		
			1.628		-0.60	-0.25		
			1.625		-0.55	-0.30	23.0	1.05
			1.628		-0.55	-0.30		
			1.625		-0.60	-0.25		
			1.627		-0.60	-0.25		

Table 5. Data for plotting velocity profile curve

No.	Point gage ft.	Dist. from bed ft.	Manometer in.	H in.	H	$v = 1.79\sqrt{H}$ fps	Tailgate	Depth of flow ft.
Material:	Cured polyester resin							
	1.505	0.000	1.500	0.000	0.000	0.000	3	0.252
1	1.515	0.010	1.821	0.321	0.566	1.013		
2	1.525	0.020	1.908	0.408	0.638	1.140		
3	1.545	0.040	1.990	0.490	0.700	1.252		
4	1.585	0.080	2.042	0.542	0.737	1.320		
5	1.625	0.120	2.076	0.576	0.758	1.357		
6	1.665	0.160	2.093	0.593	0.770	1.377		
7	1.705	0.200	2.119	0.619	0.785	1.405		
8	1.745	0.240	2.128	0.628	0.790	1.422		
9	1.757	0.252	- -	- -	- -	- -		
	1.505	0.000	1.500	0.000	0.000	0.000	2 7/8	0.228
1	1.515	0.010	1.810	0.310	0.556	0.990		
2	1.535	0.030	1.946	0.446	0.667	1.192		
3	1.555	0.050	2.040	0.540	0.734	1.312		
4	1.585	0.080	2.058	0.558	0.744	1.330		
5	1.625	0.120	2.068	0.568	0.752	1.345		
6	1.665	0.160	2.084	0.584	0.764	1.365		
7	1.705	0.200	2.113	0.613	0.783	1.405		
8	1.733	0.228	- -	- -	- -	- -		
	1.505	0.000	1.500	0.000	0.000	0.000	2 6/8	0.203
1	1.515	0.010	1.868	0.368	0.605	1.080		
2	1.525	0.020	1.908	0.408	0.638	1.140		
3	1.545	0.040	2.006	0.506	0.710	1.270		
4	1.585	0.080	2.035	0.535	0.730	1.305		
5	1.625	0.120	2.066	0.566	0.751	1.345		
6	1.665	0.160	2.089	0.589	0.765	1.370		
7	1.708	0.203	- -	- -	- -	- -		
	1.505	0.000	1.641	0.000	0.000	0.000	2 5/8	0.184
1	1.515	0.010	1.926	0.285	0.533	0.955		
2	1.525	0.020	2.014	0.373	0.610	1.090		
3	1.545	0.040	2.120	0.479	0.691	1.238		
4	1.585	0.080	2.178	0.537	0.731	1.310		
5	1.625	0.120	2.218	0.557	0.745	1.332		
6	1.665	0.160	2.228	0.587	0.764	1.365		
7	1.689	0.184	- -	- -	- -	- -		

Table 5 (Continued)

No.	Point gage ft.	Dist. from bed ft.	Manometer in.	H in.	H	$v = 1.79\sqrt{H}$ fps	Tailgate	Depth of flow ft.
	1.505	0.000	1.641	0.000	0.000	0.000	2 4/8	0.154
1	1.515	0.010	1.930	0.289	0.536	0.960		
2	1.525	0.020	1.991	0.350	0.591	1.059		
3	1.545	0.040	2.027	0.386	0.621	1.111		
4	1.565	0.060	2.053	0.412	0.641	1.149		
5	1.605	0.100	2.149	0.508	0.710	1.270		
6	1.645	0.140	2.163	0.522	0.723	1.295		
7	1.659	0.154	- -	- -	- -	- -		
	1.505	0.000	1.641	0.000	0.000	0.000	2 3/8	0.133
1	1.515	0.010	1.878	0.237	0.486	0.870		
2	1.525	0.020	1.977	0.336	0.580	1.040		
3	1.545	0.040	2.022	0.381	0.617	1.105		
4	1.565	0.060	2.080	0.439	0.651	1.165		
5	1.585	0.080	2.120	0.479	0.690	1.235		
6	1.605	0.100	2.125	0.484	0.697	1.246		
7	1.638	0.133	- -	- -	- -	1.246		
Material:		Plastic						
	1.505	0.000	1.641	0.000	0.000	0.000	3	0.184
1	1.515	0.010	1.772	0.131	0.362	0.648		
2	1.525	0.020	1.798	0.157	0.396	0.709		
3	1.545	0.040	1.836	0.195	0.442	0.790		
4	1.585	0.080	1.847	0.206	0.454	0.813		
5	1.625	0.120	1.856	0.215	0.464	0.830		
6	1.665	0.160	1.856	0.215	0.464	0.830		
7	1.689	0.184	- -	- -	- -	- -		
	1.505	0.000	1.641	0.000	0.000	0.000	2 7/8	0.165
1	1.515	0.010	1.766	0.125	0.354	0.635		
2	1.525	0.020	1.790	0.151	0.388	0.695		
3	1.545	0.040	1.821	0.180	0.424	0.760		
4	1.565	0.060	1.835	0.194	0.440	0.788		
5	1.585	0.080	1.845	0.204	0.452	0.810		
6	1.625	0.120	1.855	0.214	0.462	0.825		
7	1.670	0.165	- -	- -	- -	- -		
	1.505	0.000	1.641	0.000	0.000	0.000	2 6/8	0.147
1	1.515	0.010	1.760	0.119	0.345	0.618		
2	1.525	0.020	1.790	0.149	0.386	0.691		
3	1.545	0.040	1.832	0.191	0.437	0.783		

Table 5 (Continued)

No.	Point gage ft.	Dist. from bed ft.	Manometer in.	H in.	H	$v = 1.79\sqrt{H}$ fps	Tailgate	Depth of flow ft.
4	1.565	0.060	1.844	0.203	0.451	0.809		
5	1.585	0.080	1.848	0.207	0.455	0.815		
6	1.625	0.120	1.854	0.213	0.461	0.824		
7	1.652	0.147	- -	- -	- -	- -		
	1.505	0.000	1.641	0.000	0.000	0.000	2 5/8	0.122
1	1.515	0.010	1.741	0.100	0.316	0.566		
2	1.525	0.020	1.786	0.145	0.381	0.582		
3	1.545	0.040	1.827	0.186	0.432	0.772		
4	1.565	0.060	1.827	0.186	0.432	0.772		
5	1.585	0.080	1.837	0.196	0.442	0.790		
6	1.605	0.100	1.837	0.196	0.442	0.790		
7	1.627	0.122	- -	- -	- -	- -		
	1.505	0.000	1.641	0.000	0.000	0.000	2 4/8	0.107
1	1.515	0.010	1.760	0.119	0.345	0.618		
2	1.525	0.020	1.770	0.129	0.359	0.643		
3	1.545	0.040	1.780	0.139	0.373	0.669		
4	1.565	0.060	1.780	0.139	0.373	0.669		
5	1.585	0.080	1.790	0.149	0.385	0.690		
6	1.605	0.100	- -	- -	- -	- -		
7	1.612	0.107	- -	- -	- -	- -		
	1.505	0.000	1.641	0.000	0.000	0.000	2 3/8	0.083
1	1.515	0.010	1.724	0.083	0.288	0.516		
2	1.525	0.020	1.748	0.107	0.327	0.586		
3	1.545	0.040	1.770	0.129	0.359	0.643		
4	1.565	0.060	1.788	0.147	0.383	0.686		
5	1.585	0.080	1.788	0.147	0.383	0.686		
6	1.588	0.083	- -	- -	- -	- -		

Determination of the Equation of the Velocity Profile Curve

In Fig. 37, v is the velocity in fps., D, the depth of flow in ft. and Y, the distance from the channel bed in ft. at which the velocity is determined.

Assume a form of equation,

$$v = C \left(\frac{Y}{D}\right)^m . \qquad \text{(i)}$$

Taking logarithm of both sides,

$$\log v = \log C + m \log \left(\frac{Y}{D}\right). \qquad \text{(ii)}$$

Put $Y = \log v$

$a = \log C$

$b = m$

$X = \log \frac{Y}{D}$.

Then equation (ii) becomes,

$$Y = a - bX . \qquad \text{(iii)}$$

When Y and X are known a and b can be determined by regression technique as shown below:

$$a = \overline{Y} - b\overline{X} ,$$

where $\overline{Y} = \frac{\sum Y}{n}$, n being the number of observations of v

and $\overline{X} = \frac{\sum X}{n}$.

$$b = \frac{\sum (X - \overline{X})(Y - \overline{Y})}{\sum (X - \overline{X})^2}$$

After finding a and b, and substituting their values in

Fig. 37. Sketch of velocity profile curve, Y vs. V, where
Y = distance from bed in ft., and
V = velocity in fps.

Fig. 38. Sketch of velocity profile curve to determine v_m and v_c, where v_m = mean velocity of flow, and v_c = centroidal velocity.

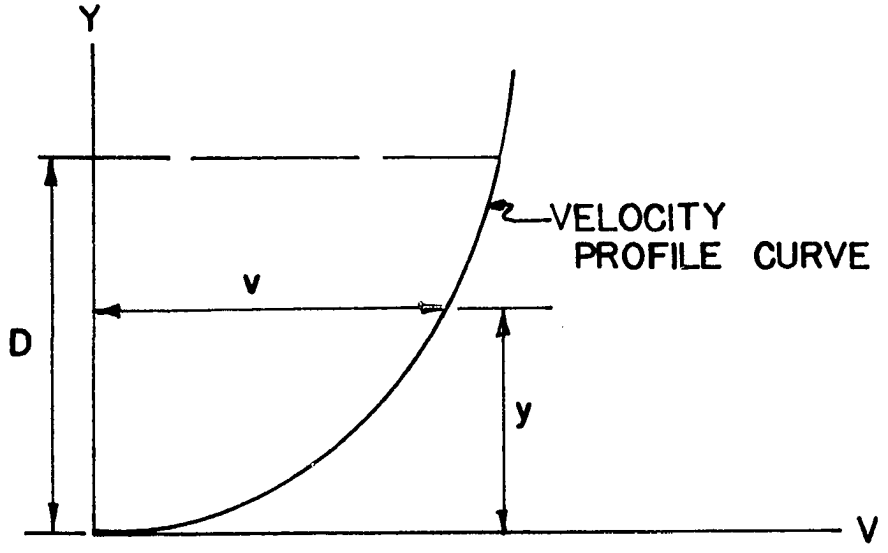
Y
VELOCITY
PROFILE CURVE
v
D
y
V

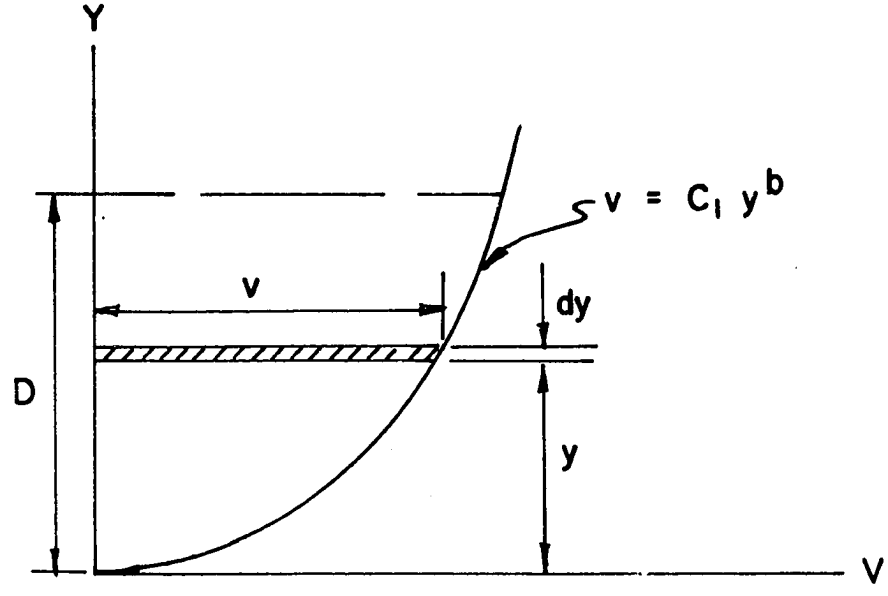
Y
v = C1 y^b
v
dy
D
y
V

(iii), antilogarithm of both sides are taken to obtain equation (i).

Table 6 shows a sample set of calculations for the determination of the equation of the velocity profile curve.

Determination of the Mean and Centroidal Velocities

Mean velocity

Equation of the velocity profile curve sketched in Fig. 38 is

$$v = a \left(\frac{y}{D}\right)^b \qquad \text{(iv)}$$

where v = velocity in fps

a = a coefficient

b = an exponent

D = depth of flow in ft.

y = distance from the bed of channel in ft.

$$dA = vdy = \frac{a}{D^b} y^b dy .$$

$$A = \frac{a}{D^b} \int_0^D y^b dy$$

$$= \frac{a}{D^b} \left[\frac{y^{b+1}}{b+1}\right]^D = \frac{a}{D^b} \left[\frac{D^{b+1}}{b+1}\right]$$

$$= \frac{a}{b+1} (D) .$$

Therefore, mean velocity for the depth D,

$$v_m = \frac{1}{D} \left[\frac{a}{b+1}\right]^D = \frac{a}{b+1} .$$

Table 6. Sample set of calculations for the determination of velocity profile curve

Y	X	ΣY	ΣX	ΣY^2	ΣX^2	ΣXY
0.00561	-1.40121					
0.05690	-1.10018					
0.09760	-0.80915					
0.12123	-0.49812					
0.13258	-0.32203					
0.13893	-0.19709					
0.14768	-0.10018					
0.15290	-0.2100					
0.15290	0.000	1.0063	-4.4507	0.1329	4.2297	-0.2979

$$\bar{Y} = \frac{\Sigma Y}{n} = \frac{1.0063}{9} = 0.1118$$

$$\bar{X} = \frac{\Sigma X}{n} = \frac{-4.4507}{9} = -0.4945$$

$$\bar{X}\Sigma X = 2.2009$$

$$\bar{X}\Sigma Y = -0.4976$$

$$b = \frac{\Sigma(X - \bar{X})(Y - \bar{Y})}{\Sigma(X - \bar{X})^2} = \frac{\Sigma XY - \bar{X}\Sigma Y}{\Sigma X^2 - \bar{X}\Sigma X}$$

$$= \frac{0.1997}{2.0288} = 0.09843$$

$$B\bar{X} = -0.04867$$

$$a = \bar{Y} - B\bar{X} = 0.1605.$$

Thus $Y = 0.1605 - 0.1190\ X$

or $\log v = 0.1605 - 0.1190 \log \left(\frac{y}{D}\right)$.

Taking antilogarithm of both sides,

$$v = 1.447 \left(\frac{y}{D}\right)^{0.119}.$$

Centroidal velocity

Refer to Fig. 35.

$$dA = vdy = \frac{a}{D^b} y^b dy \ .$$

Considering the flow to a distance d from the bed, where d = diameter of the cylinder,

$$A = \frac{a}{D^b} \int_0^d y^b dy = \frac{a}{D^b} \left[\frac{d^{b+1}}{b+1} \right]$$

$$dM_v = \frac{a}{D^b} y^{b+1} dy$$

$$M_v = \frac{a}{D^b} \int_0^d y^{b+1} dy = \frac{a}{D^b} \left[\frac{y^{b+2}}{b+2} \right]_0^d$$

$$= \frac{a}{D^b} \left[\frac{d^{b+2}}{b+2} \right]$$

$$\bar{y} = \frac{M_v}{A} = \frac{b+1}{b+2} (d) \ . \qquad (v)$$

Substitute this value for y in equation (iv)

$$v = v_c = \frac{a}{D^b} \left[\frac{b+1}{b+2} (d) \right]^b$$

where v_c = the centroidal velocity.

Determination of Velocity from Differential Manometer Reading (8)

Let H = differential manometer reading in inches of the gage fluid, and

v = velocity in fps.

Density of the gage fluid = 1.595 at 20°C.

$$v = \sqrt{2g(\gamma_{gf} - 1)\frac{H}{12}} \quad . \qquad \text{(vi)}$$

γ_{gf} = specific gravity of the gage fluid

g = acceleration due to gravity.

Substituting these values in equation (vi),

$$v = \sqrt{64.4\ (\gamma_{gf} - 1)\frac{H}{12}}$$

$$= \sqrt{64.4\ (0.595)\frac{H}{12}} = 1.79\sqrt{H} \ .$$

Table 7. Data for Fig. 36. π_1 vs. π_7 for the range of π_3 from 6.17 to 6.81[a]

π_3	π_1	π_7
6.81	0.353	3140
6.17	0.395	2690
6.40	0.392	2140
6.73	0.367	2360
6.42	0.345	1030
6.50	0.242	1240
6.44	0.234	1680
6.60	0.219	1810
6.80	0.241	1940

[a] $\pi_1 = \dfrac{L}{v_m^2 d^2}$

$\pi_7 = \dfrac{v_m d}{}$

$\pi_3 = \dfrac{D}{d}$.